Formation of Jets by Baroclinic Turbulence

Brian F. Farrell

Department of Earth and Planetary Sciences

Harvard University

Cambridge, MA 02138 *

Petros J. Ioannou

Department of Physics

National and Capodistrian University of Athens

Athens, Greece

December 7, 2007

Submitted to the Journal of the Atmospheric Sciences

*corresponding author: Brian Farrell, Harvard University, Department of Earth and Planetary Sciences, Geological Museum 452, 24 Oxford Street, Cambridge, MA 02138. email:farrell@seas.harvard.edu

ABSTRACT

Turbulent flows are frequently observed to spontaneously self organize into large spatial scale jets; geophysical examples of this phenomenon include the Jovian banded winds and the Earth's polar front jet. These relatively steady large scale jets arise from and are maintained by the much smaller spatial and temporal scale turbulence with which they coexist. Frequently these jets are found to be adjusted into marginally stable states that support large transient growth. In this work a comprehensive theory for the interaction of jets with turbulence, stochastic structural stability theory (hereafter SSST), is applied to the two-layer baroclinic model problem with the object of elucidating the physical mechanism producing and maintaining baroclinic jets, understanding how jet amplitude, structure and spacing is controlled, understanding the role of parameters such as the temperature gradient and static stability in determining jet structure, understanding the phenomenon of abrupt reorganization of jet structure as a function of parameter change, and understanding the general mechanism by which turbulent jets adjust to highly amplifying marginally stable states.

When the mean baroclinic forcing is weak, so that the mean jet is stable in the absence of turbulence, jets emerge as an instability of the coupled system consisting of the mean jet dynamics and the ensemble mean eddy dynamics. Destabilization of this coupled SSST system occurs as a critical turbulence level is exceeded. At supercritical turbulence levels the unstable jet grows at first exponentially, but eventually equilibrates nonlinearly into stable states of mutual adjustment between the mean flow and turbulence. The jet structure, amplitude and spacing can be inferred from these equilibria.

With weak mean baroclinic forcing and weak but supercritical turbulence levels the equilibrium jet structure is nearly barotropic. Under strong mean baroclinic forcing, so that the mean jet is unstable in the absence of turbulence, marginally stable highly non-normal equilibria emerge that support high transient growth and produce power law relations between heat flux and temperature gradient. The origin of this power law behavior can be traced to the

non-normality of the adjusted states.

As the stochastic excitation, mean baroclinic forcing, or the static stability are changed, meridionally confined jets that are in equilibrium at a given meridional wavenumber abruptly reorganize to another meridional wavenumber at critical values of these parameters.

The equilibrium jets obtained with the SSST system are in remarkable agreement with equilibrium jets obtained in simulations of fully developed baroclinic beta plane turbulence and the phenomenon of discontinuous reorganization of confined jets has important implications for storm track reorganization and abrupt climate change.

1. Introduction

Coherent jets that are not forced at the jet scale are often observed in turbulent flows with a familiar geophysical scale example being the banded winds of the gaseous planets (Ingersoll 1990; Vasavada and Showman 2005). The Earth's midlatitude troposphere provides example of both forced and emergent jets: although substantially modified by eddy fluxes the Earth's subtropical jets would exist in some form without these fluxes (Held and Hou 1980), while the Earth's polar front jets are essentially eddy driven (Jeffreys 1933; Lee and Kim 2003). The phenomenon of spontaneous jet organization in turbulence has been extensively investigated in observational and in theoretical studies (Rhines 1975; Williams 1979, 2003; Panetta 1993; Nozawa and Yoden 1997; Huang and Robinson 1998; Manfroi and Young 1999; Vallis and Maltrud 1993; Cho and Polvani 1996; Galperin et al. 2004; Lee 2005) as well as in laboratory experiments (Krishnamurti and Howard 1981; Read et al. 2004, 2007). The mechanism by which eddies maintain jets against surface drag is upgradient momentum flux produced by the continuous spectrum of shear waves as distinct from the discrete set of jet modes (Huang and Robinson 1998; Panetta 1993; Vallis and Maltrud 1993). This upgradient momentum transfer mechanism maintains jets in barotropic flows (Huang and Robinson 1998) and is also an important component of the forcing maintaining baroclinic jets (Panetta 1993; Williams 2003). However, baroclinic jet structure is additionally influenced by eddy heat fluxes and secondary circulations as well as by externally imposed mean thermal forcing.

A characteristic feature of jets in strong planetary scale turbulence is marginal stability coexisting with robust transient growth (Farrell 1985; Hall and Sardeshmukh 1998; Sardeshmukh and Sura 2007). The example of this phenomenon in the case of the mid-latitude troposphere is referred to as baroclinic adjustment and theories advanced to rationalize the maintenance of the mid-latitude atmosphere in marginally stable but highly non-normal states include adjustment by unstable modes themselves (Stone 1978; Held 1978; Lindzen and Farrell 1980; Gutowski 1985; Gutowski et al. 1989; Stone and Branscome 1992; Lindzen 1993; Welch and Tung 1998; Zurita-Gotor and Lindzen 2004a,b; Schneider and Walker 2006) and turbulence transport scaling arguments (Zhou and Stone 1993; Held and Larichev 1996; Held 1999; Zurita-Gotor 2007). Besides marginal stability and high non-normality these ad-

justed states are also characterized by power law behavior of fluxes as a function of stability parameters such as the temperature gradient (Held and Larichev 1996; Barry et al. 2002; Zurita-Gotor 2007).

We show using stochastic structural stability theory (SSST) how the atmosphere adjusts to the observed stable but highly amplifying mean states. Analogous behavior often arises when a feedback controller is imposed to stabilize multidimensional mechanical or electronic systems and attempts to suppress the non-normal growth in such systems gave rise to robust control theory (Zhou and Doyle 1998). It is commonly held in the robust control community (Doyle; private communication) that stable but fragile equilibria are unnatural, arising only as a consequence of the design process (Bobba et al. 2007). We maintain that in the case of the eddy driven jets the state of high non-normality together with marginal stability is inherent because turbulence maintains flow stability with a naturally occurring feedback controller. A fundamental advantage of SSST is that it clearly reveals the feedback stabilization process and how it places the system in a stable but highly amplifying state.

Excitation of the turbulent eddies can be traced either to exogenous short time scale processes such as convection, as in the case of the Jovian jets, or to endogenous turbulence generated internally, as in the case of the Earth's polar front jet. Because in either case these processes have short time and space scales compared to the jet time and spatial scale, the wave forcing can be modelled stochastically. The central component of a theory for the dynamics of jets in turbulence, the method to obtain the structure of the turbulence and the associated fluxes given the jet, is provided by stochastic turbulence modelling (Farrell and Ioannou 1993c, 1994, 1995, 1996; DelSole and Farrell 1995; DelSole 1996; DelSole and Farrell 1996; Newman et al. 1997; Whitaker and Sardeshmukh 1998; Zhang and Held 1999; DelSole 2004b). Once these fluxes are known the equilibrium states of balance among the large scale thermal forcing the friction and the ensemble mean turbulent flux divergences can be determined; this is the method of SSST (Farrell and Ioannou 2003, 2007). The interaction between large scale jet structure and the field of eddy turbulence is nonlinear and results in a nonlinear trajectory that often tends to an equilibrium, sometimes to a limit cycle and under extraordinary conditions is chaotic.

The three length scales in the baroclinic dynamics of the two layer model on a beta plane

are the scale imposed by the boundaries, the Rhines scale $L_\beta = \sqrt{U/\beta}$ and the Rossby radius $L_R = NH/f_0$, in which f_0 is the Coriolis parameter, β its meridional gradient, N the buoyancy frequency, H the depth of the fluid and U a characteristic velocity. Emergence of any of these length scales in the solution can not be used to argue for any particular physical mechanism maintaining the jets because the intrinsic scales of the problem are common to all mechanisms and can at best be used to argue consistency with the dynamics. The Rhines radius is the characteristic scale of eddy driven jets (Panetta 1993) and it is a fundamental theoretical problem to identify the physical mechanism producing this scale from the dynamics.

We find that in the presence of turbulence and even in the absence of an imposed mean thermal forcing that there is a linear instability of the coupled turbulence/mean flow system giving rise to zonal jets. This jet forming instability is an example of a new class of instability in fluid dynamics; it is an emergent instability that arises essentially from the interaction between the mean flow and the turbulence. The modal jet perturbation growth rate is at first exponential because at sufficiently small amplitude the jet modes organize the turbulence field to produce fluxes proportional in magnitude and consistent in structure with the jet mode.

It is instructive to consider this jet forming instability as a function of the strength of the stochastic excitation, the mean thermal forcing and the static stability while recognizing that dissipation could also be added to this list.

With sufficiently energetic stochastic excitation and no mean thermal forcing nearly barotropic zonal jets emerge spontaneously. If the stochastic excitation is not too strong these jets nonlinearly equilibrate, in balance with dissipation, with nearly sinusoidal barotropic structure. However, as the stochastic excitation is increased, the nonlinearly balanced jets increase in amplitude and encroach on eddy stability boundaries. This results in modification of the jet structure as SSST fixed point equilibria enforce stability of the jet to eddy perturbations because eddy fluxes diverge at stability boundaries[1]. To avoid instability the

[1]It is logically necessary that exponential eddy instabilities be equilibrated in some manner. The mechanism of equilibration in our model, and we believe the primary mechanism in atmospheric jets generally, is through modification of the mean jet structure by the eddy fluxes. In our quasigeostrophic model this modification is necessarily confined to changes in jet velocity and attendant horizontal temperature gradients but more generally modification of static stability must be involved in some manner that remains to be

jets become increasingly east/west asymmetric with the westward jet equilibrating primarily barotropically at the Rayleigh-Kuo scale which is essentially the Rhines radius.

When mean thermal forcing is imposed baroclinic equilibria are found; under strong stochastic excitation the eastward-portion of these jets equilibrate maintaining perturbation eddy stability by meridional confinement while supporting substantial baroclinicity (Ioannou and Lindzen 1986; James 1987; Roe and Lindzen 1996) while the westward portions equilibrate barotropically near the Rayleigh-Kuo boundary.

If the jets are quantized by meridional boundaries, as would be the case for a planet of finite radius, a discontinuous reorganization of structure is induced at threshold parameter values for which stable equilibrium states of the extant marginally stable wavenumber cease to exist. This provides an instructive example of the general phenomenon of eddy driven jets appearing and disappearing discontinuously as a function of slow parameter change (Farrell and Ioannou 2003; Robinson 2006). While understanding the physical mechanism of the eddy driven jet is a fundamental GFD problem, it also has important climate connections because this mechanism of discontinuous reorganization of eddy driven jets can alter both climate statistics, by altering storm tracks and the source regions associated with isotopic signatures (Alley et al. 1993; Fuhrer et al. 1999; Wunsch 2003) and the climate itself, by changing the latitude of surface stresses and associated oceanic upwelling (Toggweiler et al. 2006). This mechanism for abrupt change of climate and climate statistics arising from storm track reorganization joins the short list of reorganization of thermohaline ocean circulations (Weaver et al. 1991) and sea-ice switches (Gildor and Tziperman 2003; Li et al. 2005) as possible mechanisms for explaining the observed record of abrupt climate change.

In this work we study the structure and dynamics of jets in baroclinic turbulence by joining the equation governing the stochastically forced perturbation field with the equation for the zonal mean to form a coupled wave-mean flow evolution system. This nonlinear coupled equation system is the basic tool of SSST analysis and we have applied it previously to the study of barotropic jets (Farrell and Ioannou 2003, 2007).

---

investigated.

2. Dynamics of the zonally averaged velocity in turbulent flows

a. Formulation

A theory for jet dynamics in turbulent flow was developed in Farrell and Ioannou (2003). This theory was applied to the problem of the formation of jets in barotropic turbulence in (Farrell and Ioannou 2007). Here we provide a brief review of the salient ideas of this theory in the context of baroclinic jets which is the focus of this work.

Consider a turbulent rotating two layer baroclinic fluid on the $x-y$ plane and let $U_{1,2}(y,t)$ be the latitudinally (y) and time (t) dependent mean velocities of the upper (denoted as 1) and lower (denoted as 2) layers, the mean being taken in the zonal (x) direction. The barotropic (denoted $+$) and baroclinic (denoted $-$) mean flows defined as

$$U^+ = \frac{U_1 + U_2}{2} \quad , \quad U^- = \frac{U_1 - U_2}{2} \quad , \tag{1}$$

obey the following evolution equations (DelSole and Farrell 1996; Valis 2006):

$$U_t^+ = -\frac{\overline{r}_2}{2}(U^+ - U^-) + F^+ \tag{2}$$

$$(D^2 - 2\lambda^2)U_t^- = \frac{\overline{r}_2}{2}D^2(U^+ - U^-) - 2r_R\lambda^2(U_R^- - U^-) + F^- \tag{3}$$

in which the terms proportional to $\overline{r}_2$ represents linear damping of the mean flow at the lower layer (layer 2) to a state of rest at the mean rate $\overline{r}_2$ (we assume no Rayleigh damping in the upper layer); the term proportional to r_R represents linear relaxation of the baroclinic flow to the imposed baroclinic flow U_R^- at the mean rate of the coefficient of Newtonian cooling r_R; the terms F^+ and F^- (explicit forms given later) represent the forcing of the zonal flow by the eddies. The non-dimensional Rossby radius of deformation is $1/\lambda = NH/fL$ where L is the horizontal scale, H the height of each layer, N the static stability and f the coriolis parameters. The operator $D^2 \equiv \partial^2/\partial y^2$.

The mean equation are written in the compact form

$$\frac{\partial \mathbf{U}}{\partial t} \;=\; \mathbf{G}\mathbf{U} \;+\; \mathbf{H}. \tag{4}$$

in which the $\mathbf{U}$ is the full mean state velocity vector:

$$\mathbf{U} \;\equiv\; \begin{pmatrix} U^{+} \\ U^{-} \end{pmatrix} \;\;, \tag{5}$$

$\mathbf{G}$ is the linear dynamical operator:

$$\mathbf{G} \;=\; \begin{pmatrix} \mathbf{G}_{11} & \mathbf{G}_{12} \\ \mathbf{G}_{21} & \mathbf{G}_{22} \end{pmatrix} \tag{6}$$

with components:

$$\mathbf{G}_{11} \;=\; -\frac{\overline{r}_2}{2} \;\;, \tag{7.a}$$

$$\mathbf{G}_{12} \;=\; \frac{\overline{r}_2}{2} \;\;, \tag{7.b}$$

$$\mathbf{G}_{21} \;=\; (D^2 - 2\lambda^2)^{-1}\left(\frac{\overline{r}_2}{2} D^2\right) \;\;, \tag{7.c}$$

$$\mathbf{G}_{22} \;=\; (D^2 - 2\lambda^2)^{-1}\left(-\frac{\overline{r}_2}{2} D^2 \;+\; 2r_R\lambda^2\right) \;, \tag{7.d}$$

and the mean flow forcing H is composed of the eddy forcing and the mean thermal relaxation toward the radiative equilibrium thermal wind U_R^-:

$$\mathbf{H} \;\equiv\; \begin{pmatrix} F^{+} \\ (D^2 - 2\lambda^2)^{-1}\left(D^2 F^{-} - 2r_R\lambda^2 U_R^{-}\right) \end{pmatrix} \tag{8}$$

The eddy forcing of the mean flow is expressed in terms of the barotropic and baroclinic eddy streamfunction (DelSole and Farrell 1996; Valis 2006) as:

$$F^{+} \;=\; \overline{\psi_x^{+}\psi_{yy}^{+} + \psi_x^{-}\psi_{yy}^{-}} \;\;, \tag{9.a}$$

$$F^{-} \;=\; \overline{\psi_x^{+}\psi_{yy}^{-} + \psi_x^{-}\psi_{yy}^{+} - 2\lambda^2\psi_x^{+}\psi^{-}} \;\;. \tag{9.b}$$

The overbars denote zonal averaging and the zonal and meridional barotropic and baroclinic component of the perturbation velocities are related to the y and x derivatives of the streamfunctions $\psi^{\pm}$ as:

$$u^{\pm} \;=\; -\,\psi^{\pm}_{y} \quad , \qquad v^{\pm} \;=\; \psi^{\pm}_{x} \quad . \tag{10}$$

The perturbation streamfunctions are written as a Fourier sum of zonal harmonics:

$$\psi^{\pm}(x,y,t) = \sum_{k} \psi^{\pm}_{k}(y,t) e^{ikx} \; . \tag{11}$$

The zonal average $\overline{ab}$ of the product of two sinusoidally varying fields $\hat{a}\; e^{ikx}$ and $\hat{b}\; e^{ilx}$ is $\mathrm{Re}(\hat{a}\hat{b}^{*})\delta_{kl}/2$ ($*$ denotes complex conjugation). Using this property we can express the eddy forcings (9.a, 9.b) in terms of the eddy streamfunction Fourier amplitudes as:

$$F^{+} \;=\; -\;\sum_{k}\;\frac{k}{2}\;\mathrm{Im}\left(\;\psi^{+}_{k} D^{2}\psi^{+*}_{k} \;+\; \psi^{-}_{k} D^{2}\psi^{-*}_{k}\right) \quad , \tag{12.a}$$

$$F^{-} \;=\; -\;\sum_{k}\;\frac{k}{2}\;\mathrm{Im}\left(\;\psi^{+}_{k} D^{2}\psi^{-*}_{k} \;+\; \psi^{-}_{k} D^{2}\psi^{+*}_{k} \;-\; 2\lambda^{2}\psi^{+}_{k}\psi^{-*}_{k}\right) \quad . \tag{12.b}$$

Each Fourier component of the perturbation streamfunction evolves according to the stochastically excited linear equation:

$$\frac{\partial}{\partial t}\begin{pmatrix} \psi^{+}_{k} \\ \psi^{-}_{k} \end{pmatrix} \;=\; \mathbf{A}_{k}(\mathbf{U}) \begin{pmatrix} \psi^{+}_{k} \\ \psi^{-}_{k} \end{pmatrix} \;+\; \mathbf{P}_{k} \begin{pmatrix} \xi(t)^{+} \\ \xi(t)^{-} \end{pmatrix} \tag{13}$$

In (13) the second term on the r.h.s. represents stochastic excitation and the first term is the autonomous linear operator of the perturbation dynamics:

$$\mathbf{A}_{k}(\mathbf{U}) \;=\; \begin{pmatrix} \mathbf{A}^{+}_{k}(\mathbf{U}^{+}) & \mathbf{A}^{+}_{k}(\mathbf{U}^{-}) \\ \mathbf{A}^{-}_{k}(\mathbf{U}^{+}) & \mathbf{A}^{-}_{k}(\mathbf{U}^{-}) \end{pmatrix} \tag{14}$$

in which the individual linear operators are:

$$\mathbf{A}_k^+(\mathbf{U}^+) \;=\; \Delta^{-1}\left(-ik\mathbf{U}^+\Delta \;-\; ik\left(\beta - D^2\mathbf{U}^+\right)\right) \;-\; r^+ - r_{eff} \quad , \tag{15.a}$$

$$\mathbf{A}_k^+(\mathbf{U}^-) \;=\; \Delta^{-1}\left(-ik\mathbf{U}^-\Delta \;+\; ikD^2\mathbf{U}^-\right) \;-\; r^- \quad , \tag{15.b}$$

$$\mathbf{A}_k^-(\mathbf{U}^+) \;=\; (\Delta - 2\lambda^2)^{-1}\left(-ik\mathbf{U}^-\left(\Delta \;+\; 2\lambda^2\right) \;+\; ikD^2\mathbf{U}^- \;-\; r^-\Delta\right) \quad , \tag{15.c}$$

$$\mathbf{A}_k^-(\mathbf{U}^-) \;=\; (\Delta - 2\lambda^2)^{-1}\left(-ik\mathbf{U}^+\left(\Delta \;-\; 2\lambda^2\right) \;+\; \left(\beta - D^2\mathbf{U}^+\right) \;-\; r^+\Delta \;+\; 2r_R\lambda^2\right) \;-\; r_{eff} \quad , \tag{15.d}$$

in which $\Delta \equiv D^2 - k^2$ the Laplacian and Δ^{-1} the inverse of the Laplacian in which the appropriate lateral boundary conditions have been incorporated. In writing (13) we have included in the linear operator parameterization of the non-linear terms in the complete perturbation equation as stochastic excitation and added dissipation in the form of linear damping of the streamfunction at rate r_{eff} (Farrell and Ioannou 1993b, 1996; DelSole and Farrell 1996; Newman et al. 1997; DelSole 2004b). The coefficients $r^{\pm}$ are the linear damping rates of the barotropic and baroclinic streamfunction respectively.

The stochastic excitation is given by

$$\mathbf{P}_k \;=\; \alpha_k \begin{pmatrix} \Delta^{-1} & 0 \\ 0 & (\Delta - 2\lambda^2)^{-1} \end{pmatrix} \begin{pmatrix} \mathbf{W}^+(y) & 0 \\ 0 & \mathbf{W}^-(y) \end{pmatrix} \quad , \tag{16}$$

The stochastic excitation of the potential vorticity represented by (16) is delta correlated in time and spatially correlated by $\mathbf{W}^{\pm}(y)$ which is chosen to give a numerically resolved representation of localized excitation. The scalar coefficient α_k is chosen so that each perturbation wavenumber is forced with equal energy.

The continuous operators are discretized and the dynamical operator is approximated by a finite dimensional matrix. The state $\psi^{\pm}(k)$ is represented by a column vector with entries the complex value of the streamfunction at collocation points. In this approximation $\mathbf{W}_k$ represents the spatial (y) correlation in the stochastic excitation. Care must be taken that the structure of excitation matrix $\mathbf{W}_k$ doesn't bias the response. We select $\mathbf{W}_k$ matrices producing Gaussian autocorrelation function about the level of excitation y_i proportional to

$\exp(-(y-y_i)^2/\delta^2)$ so that δ controls the correlation distance in y. This forcing matrix is the same for all zonal wavenumbers.

If the layers are excited equally the stochastic excitation of the time dependence of the barotropic $\xi^+(t)$ and baroclinic $\xi^-(t)$ components is equal and statistically independent so that

$$< \xi^+(t)\xi^{-\dagger}(t) >= \mathbf{O}. \tag{17}$$

We choose each of the excitations to be delta correlated white noise with zero mean and unit variance:

$$< \xi^+(t) >=< \xi^-(t) >= 0 \quad , \; < \xi^+(t)\xi^{+\,\dagger}(s) >=< \xi^-(t)\xi^{-\,\dagger}(s) >= \mathbf{I}\,\delta(t-s) \quad , \tag{18}$$

where $\mathbf{I}$ is the identity matrix. The brackets denote an ensemble average, i.e. an average over realizations of the forcing. If only the upper layer is forced then the barotropic and baroclinic forcing are taken equal to $\xi^+(t)$.

The system consisting of (4) and (13) describes the dynamics of a single realization of a stochastically excited wave interacting with the jet. This system results in strong fluctuations in jet structure. However, there are usually many independently excited waves simultaneously interacting with the jet so that the fluctuations in jet structure are suppressed by the ensemble averaging of these independently excited waves. With this assumption of ensemble average eddy forcing the time evolution of the ensemble average covariance matrix of the perturbation field

$$\mathbf{C}_k \;=\; \begin{pmatrix} \mathbf{C}_k^+ & \mathbf{C}_k^\pm \\ (\mathbf{C}_k^\pm)^\dagger & \mathbf{C}_k^- \end{pmatrix} \;, \tag{19}$$

with $\mathbf{C}_k^+ =< \psi_k^+\psi_k^{+\dagger} >$, $\mathbf{C}_k^- =< \psi_k^-\psi_k^{-\dagger} >$ and $\mathbf{C}_k^\pm =< \psi_k^+\psi_k^{-\dagger} >$, obeys the deterministic equation:

$$\frac{d\mathbf{C}_k}{dt} \;=\; \mathbf{A}_k(\mathbf{U})\mathbf{C}_k \;+\mathbf{C}_k\mathbf{A}_k^\dagger(\mathbf{U}) \;+\; \mathbf{Q}_k \;, \tag{20}$$

with

$$\mathbf{Q}_k \;=\; |\alpha_k|^2 \begin{pmatrix} \Delta^{-1}\mathbf{W}^+(\mathbf{W}^+)^\dagger\Delta^{-1\dagger} & 0 \\ 0 & (\Delta-2\lambda^2)^{-1}\mathbf{W}^-(\mathbf{W}^-)^\dagger(\Delta-2\lambda^2)^{-1\dagger} \end{pmatrix} \;, \tag{21}$$

the spatial covariance matrix for equal stochastic excitation of both layers (in case the excitation is limited to the upper layer the covariance is modified appropriately) (Farrell and Ioannou 2003). For our purposes the matrix $\mathbf{Q}_k$ includes all the relevant characteristics of the stochastic excitation: the meridional distribution of the forcing is given by the diagonal elements of this matrix and the autocorrelation function by the rows.

The ensemble mean baroclinic and barotropic eddy forcings (12.a,12.b) are expressed in terms of the covariances as:

$$< F^+ > \quad = \quad \sum_k \; -\frac{k}{2} \, \mathrm{diag}\left(\mathrm{Im}(\mathbf{C}_k^+ + \mathbf{C}_k^-) D^{2\dagger}\right) \quad , \tag{22.a}$$

$$< F^- > \quad = \quad \sum_k \; -\frac{k}{2} \, \mathrm{diag}\left(\mathrm{Im}\left((\mathbf{C}_k^\pm + \mathbf{C}_k^{\pm\dagger}) D^{2\dagger} - 2\lambda^2 \mathbf{C}_k^\pm\right)\right) \quad . \tag{22.b}$$

This ensemble mean of the zonally averaged eddy forcing approaches at each wavenumber k the zonally averaged forcing for sufficiently large number of independent realizations with arbitrary phase difference. In this limit:

$$< F^\pm >= F^\pm \; , \tag{23}$$

and the evolution equations for the covariances, (20), the equation for the eddy induced accelerations, (22.a , 22.b), and the Reynolds-averaged equations for the barotropic and baroclinic mean zonal flow, (4), define a closed autonomous nonlinear system for the evolution of the mean flow under the influence of its consistent field of turbulent eddies. This system is globally stable and energetically consistent. For typical earth values of mean baroclinic forcing, there is a small energy input by the stochastic forcing while the dominant energy balance is between energy extracted from the mean by baroclinic processes and energy lost to frictional dissipation. Typically the equilibrium solutions of this system are steady mean flows maintained with constant structure by eddy forcing although limit cycle and chaotic trajectories are found for some parameter values (Farrell and Ioannou 2003).

This ideal limit (23) in which the ensemble average is equal to the zonal average is of particular interest because in this limit, although the effect of the ensemble average turbulent fluxes is retained in the solution, the fluctuations associated with the turbulent eddies are

suppressed by the averaging and the coupled jet/turbulence dynamics becomes deterministic. In this limit the mean zonal flow equilibria emerge with great clarity. With the ensemble average interpreted as a zonal average, this ideal limit is approached when the autocorrelation scale of the perturbation field, l, is much smaller than the zonal extent, L, of the channel. In that case taking the zonal average is equivalent to averaging $N = O(L/l)$ statistically independent realizations of the forcing which as $N \to \infty$ converges to the ensemble average (Farrell and Ioannou 2003). Examples of physical systems in which this limit applies include the Jovian upper atmosphere and the solar convection zone, both forced by relatively small scale convection. An experiment in which a jet emerged from rather coarse grained turbulent convection was reported by Krishnamurti and Howard (1981). When this large ensemble limit is not approached sufficiently closely the system exhibits stochastic fluctuations about the ideal equilibria. The ideal equilibrium may nevertheless be detected underlying the noisy observations using statistical methods (Koo et al. 2002). A physical system that exhibits such behavior is the Earth's polar jet. In that case the eddy dynamics is dominated by global wavenumbers 4- 10 and the number of independent systems that are averaged over a latitude circle is at most order 10, which is too small for the ideal dynamics to be realized closely so that while the underlying order is revealed by the ideal dynamics the observed zonal jet exhibits stochastic fluctuations about the ideal jet (Farrell and Ioannou 2003).

A limitation of our analysis is the assumption that the stochastic excitation is independent of the mean and eddy fields. While for the Jovian atmosphere this is probably a good assumption because the stochastic excitation is thought to arise from internally generated convection, it is a crude assumption for the Earth's polar jet where the excitation distribution parameterized by $\mathbf{Q}_k$ is influenced by the jet structure and eddy amplitude itself. Obtaining the stochastic excitation consistent with the turbulence supported by a jet is equivalent to obtaining a closure of the turbulent system. Progress on this problem has been made (DelSole and Farrell 1996; DelSole 1999). While an attractive avenue for future study, such a closure is not necessary for understanding the basic dynamics underlying emergence of zonal jets in turbulence and in the interest both of simplicity and of clarity of exposition we for the present retain a spatially uniform excitation.

b. Scaling of the equations, boundary conditions and parameters

We non-dimensionalize the equations choosing the Earth day for the time scale, t_d = 1 day, and length scale $L = 10^6$ m. All variables will henceforth be considered non-dimensional. The scale of the velocity is $L/t_d = 11.6$ ms^{-1}. The calculations are performed in a periodic channel $L_y = 20$ units wide in the meridional directions. The size of the channel has been selected wide enough to accommodate a number of jets, however, quantization effects do become important as will be shown below. The calculations use typically 64 point discretization in the meridional direction and 14 waves in the zonal direction consisting of global zonal wavenumber 1 to 14 in a reentrant zonal channel of nondimensional length $Lx = 40$.

The strength of the stochastic excitation, $\mathbf{Q}$, is measured by the forcing density f = trace($\mathbf{MQ}$)/n where $\mathbf{M}$ is the energy metric

$$\mathbf{M} \;=\; \frac{1}{2n}\begin{pmatrix} \Delta & 0 \\ 0 & (\Delta - 2\lambda^2) \end{pmatrix} \tag{24}$$

defined so that $(\psi_k^+, \psi_k^-)\mathbf{M}(\psi_k^+, \psi_k^-)^\dagger$ is the total energy per unit mass of state (ψ_k^+, ψ_k^-) at each zonal wavenumber k and n is the number of discretization points in the meridional direction. We express the stochastic excitation in dimensional units (mW kg^{-1}).

Unless otherwise specified friction parameters for the perturbation dynamics are as follows: $r_R = 1/15$, $r_2 = 1/5$, $r_{eff} = 1/20$. For the mean dynamics: $\overline{r}_2 = 1/5$, $\nu = \delta y^2$ where δy is the grid size. The Froude number in most of the calculations is $\lambda^2 = 1$.

For simplicity and to facilitate interpretation we impose meridionally homogeneous stochastic excitation and consider meridionally constant radiative equilibrium mean flows

$$U_R^{\pm} = \frac{R\Delta T}{f_0}\frac{t_d}{20L^2} \quad , \tag{25}$$

where ΔT is the temperature difference across 10^4 km and $f_0 = 10^{-4}$ 1/s is the Coriolis parameter and $R = 287$ J/(kgK) is the gas constant . These flows become baroclinically unstable when $\Delta T > \Delta T_c$ which with the above dissipation parameters is $\Delta T_c = 28.3$ K/(10^4km).

3. Stability analysis of the ensemble mean coupled system

Recall that the ensemble mean evolution is governed by the coupled equations:

$$\frac{d\mathbf{C}_k}{dt} = \mathbf{A}_k(\mathbf{U})\mathbf{C}_k + \mathbf{C}_k\mathbf{A}(\mathbf{U})^\dagger + \mathbf{Q}_k \tag{26a}$$

$$\frac{\partial \mathbf{U}}{\partial t} = \mathbf{G}\mathbf{U} + \mathbf{H}. \tag{26b}$$

This set of equations typically possesses equilibria consisting of an equilibrium velocity $\mathbf{U}^E$ and associated perturbation covariance $\mathbf{C}^E$ satisfying:

$$\mathbf{A}_k(\mathbf{U}^E)\mathbf{C}_k^E + \mathbf{C}_k^E\mathbf{A}(\mathbf{U}^E)^\dagger = -\mathbf{Q}_k \tag{27a}$$

$$\mathbf{G}\mathbf{U}^E + \mathbf{H} = 0. \tag{27b}$$

If stable these equilibria may be found by forward integration of the coupled equations (26a, 26b); otherwise, a root finder must be employed.

Two distinct concepts of jet stability arise in connection with SSST equilibria. The first is the familiar eddy perturbation stability determined by analysis of the operator $\mathbf{A}^E$. An SSST equilibrium mean flow $\mathbf{U}^E$ is by necessity stable in this sense because otherwise the eddy variance would not be finite. The converse however is not true; the stability of $\mathbf{A}^E$ does not imply the stability of the SSST equilibrium ($\mathbf{U}^E$, $\mathbf{C}^E$) and there is a new stability concept arising from the interaction of the jet with its eddy flux divergences. The stability of the coupled system (26a, 26b) is determined by analysis of the operator that governs the perturbation dynamics of the equilibria of the system (26a, 26b) as discussed in Farrell and Ioannou (2003, 2007). This structural stability of an equilibrium state depends on the strength of the stochastic excitation, $\mathbf{Q}$, the thermal forcing measured by the temperature difference ΔT, the Froude number λ^2, and the dissipation. We primarily examine the structural stability of equilibrium states as a function of $f = \text{trace}(\mathbf{M}\mathbf{Q})/n$ and ΔT.

For $\Delta T < \Delta T_c$ the radiative equilibrium flows $U_R^{\pm}$ are fixed points of the coupled system

(26a, 26b) for any stochastic excitation f because the eddy fluxes are meridionally constant. For $\Delta T > \Delta T_c$ and in the absence of stochastic excitation (in order to obtain statistical equilibria with finite eddy amplitude) the radiative equilibrium flows $U^*_\pm$ are fixed points of the coupled system (26a, 26b) . We wish to examine the structural stability of these radiative equilibria fixed points and thereby determine the conditions under which zonal jets emerge. When $\Delta T < \Delta T_c$ the radiative equilibrium $U^*_\pm$ is structurally unstable only when the stochastic excitation f exceeds a critical value f_c. When $\Delta T > \Delta T_c$ the radiative equilibrium $U^*_\pm$ is structurally unstable for all f.

In Fig. 1 this critical value of stochastic forcing f_c (mW kg^{-1}) is plotted as a function of ΔT. Because of the meridional homogeneity of the equilibrium state the perturbation eigenmodes are harmonic. Unstable jet perturbations of harmonic form with different meridional wavenumber emerge as f exceeds f_c. In Fig. 1 are shown the critical forcings required in order to obtain zonal flows with meridional wavenumbers $n = 1, .., 4$.

When the radiative equilibria are structurally unstable zonal jets ultimately equilibrate as finite amplitude extensions of the unstable eigenmodes of the coupled SSST system. These equilibria may or may not be stable fixed points, and when unstable the jets may settle in a limit cycle having periodic behavior, also chaotic trajectories are possible (Farrell and Ioannou 2003, 2007). However over a significant parameter range structurally stable fixed points are found, and these are the subject of our study in this paper.

4. Examples of jet equilibria

a. Jet equilibria with no mean thermal forcing

The equilibria found in the absence of mean thermal forcing are for a wide choice of realistic parameter values nearly barotropic and similar to those discussed in Farrell and Ioannou (2007) although with appropriate parameter choice and vertical asymmetry of stochastic excitation substantial baroclinicity can be maintained.

For supercritical stochastic excitation multiple equilibria differing in jet meridional wavenumber exist at $\Delta T = 0$ as indicated in Fig. 1 .

Examples of meridional wavenumber 2 jet equilibria are shown in Fig 2 for two different choices of stochastic excitation. In the first case the stochastic excitation is $f = 5.8$ mWkg^{-1} per wavenumber (Fig 2 a) and in the second the stochastic excitation is $f = 55.8$ mWkg^{-1} per wavenumber (Fig 2 b). The first case is stochastically excited with sufficient energy input rate to clearly show departure from the nearly harmonic equilibrium form obtained for slightly supercritical forcing. The second state is excited at a rate that places the equilibrium state close to the structural stability boundary just before the bifurcation to meridional wavenumber 1 equilibria as a function of forcing level and therefore the second equilibrium state departs maximally from the harmonic equilibrium state that results for slightly supercritical excitation.

In these examples the eddy field comprises 14 zonal wavenumbers. Although the lower layer is Ekman damped the equilibria are nearly barotropic and equilibrate close to the Rayleigh-Kuo stability boundary implying the Rhines radius for the jet scale and pronounced asymmetry between the easterly and westerly jets (Farrell and Ioannou 2007). The mean potential vorticity gradient is positive almost everywhere as shown in Fig 2. Laboratory experiments using a stratified fluid in a rotating channel with a sloping bottom verify the formation of such stable persistent mean jets when there is no mean baroclinic forcing (Read et al. 2004, 2007). The equilibrated flows although stable are highly non-normal and their non-normality increases from 53.9 to 155 as the structural stability boundary is approached. The measure of non-normality we use is the ratio of the variance maintained by stochastic excitation of this system to the variance maintained in the equivalent normal system that has the same eigenvalues but orthogonal eigenvectors when both are forced by the same stochastic excitation $\mathbf{Q} = \mathbf{I}$ (Farrell and Ioannou 1996).

These equilibria are essentially the same as were found for the barotropic problem (Farrell and Ioannou 2007) so that we may conclude that with weak stochastic excitation the baroclinic problem bifurcates from the zero state flow barotropically.

b. Jet equilibria with mean thermal forcing

Consider stochastically excited baroclinic flow. As the thermal forcing increases jets equilibrate that are marginally stable and highly non-normal. Examples of such baroclinically adjusted jets are shown in Fig. 3 a for two different levels of stochastic excitation $f = 0.48$ mW kg^{-1} and $f = 1.34$ mW kg^{-1} with mean thermal forcing $\Delta T = 30$ K/10^{4}km (recall the stability boundary is $\Delta T_c = 28.3$K/(10^{4}km)). Shown are meridional wavenumber 3 jet equilibria. The second equilibrium in Fig. 3b is close to the structural stability boundary just before the bifurcation to meridional wavenumber 2 equilibria as a function of forcing.

These westerly jets can be highly baroclinic because baroclinicity of the westerly jet increases the already positive potential vorticity gradient unlike the case of the easterly jets for which the baroclinic shear is suppressed to preserve stability as can be seen in Fig. 3 c,d. The potential vorticity gradient of the mean flow changes sign and therefore violates the Charney-Stern stability condition. The baroclinically adjusted states are primarily equilibrated by meridional confinement interacting with dissipation (Ioannou and Lindzen 1986; James 1987; Roe and Lindzen 1996).

c. Jet equilibria with barotropically unstable upper level jet equilibria

Observations of the Jupiter upper level winds show westward jets that satisfy the Rayleigh-Kuo necessary conditions for instability. These jets might be stable because for an unspecified reason a perturbation free lower layer flow exists that is configured to enforce stability (Dowling 1994). Alternatively, we find strong stable jets satisfying Rayleigh-Kuo necessary conditions for instability in their upper layers form spontaneously as equilibria with sufficient dissipation.

As an example consider the two layers with β a fifth of the terrestrial β, symmetric eddy damping $r_1 = r_2 = 1$ d^{-1}, eddy cooling of $r_R = 1/15$ d^{-1}, and dissipation of the mean $\overline{r}_1 = \overline{r}_2 = 1/250$ d^{-1} with stochastic excitation of only the upper layer at level $f = 0.972$ mWkg^{-1}. Shown are the jet profiles in the upper and lower layers together with the upper and lower layer mean potential vorticity gradients (thick and thin continuous lines

in bottom panel of Fig. 4):

$$Q_{1y} = \beta - U_1'' + \lambda^2(U_1 - U_2) \quad , \quad Q_{2y} = \beta - U_2'' - \lambda^2(U_1 - U_2) \; . \tag{28}$$

Also shown in the same figure are the barotropic vorticity gradients $\beta - U_i''$ (thick and thin dashed lines). The equilibrium jet is baroclinic with the upper level flow violating Rayleigh-Kuo stability condition by ten beta.

5. Scaling laws, baroclinic adjustment and the role of non-normality

SSST equilibrium jets that form in strong turbulence are adjusted to marginal stability. These states while stable are highly non-normal supporting large transient perturbation amplification. One consequence of this stability and non-normality in the Earth's midlatitude atmosphere is the association of cyclone formation with the chance occurrence in the stochastic turbulence of optimal or near optimal initial conditions (Farrell 1982, 1989; Farrell and Ioannou 1993c; DelSole 2004a). These optimal perturbations are analogous to the dangerous inputs that render feedback stabilized mechanical and electronic systems fragile (Zhou and Doyle 1998). In addition to explaining the stability, high non-normality and the centrality of transient growth in jet dynamics, these equilibria provide an explanation for the universal scaling laws for fluxes as a function of parameters influencing jet stability.

To introduce this last idea consider the linear dynamics of streamwise rolls in an unbounded shear flow with rotation in the roll normal direction. This system is governed by the Reynolds matrix which provides a convenient example of a dynamical system in which stability and non-normality interact:

$$\mathbf{A} \; = \; \begin{pmatrix} -\nu(l^2+m^2) & -(\alpha - 2\Omega) \\ -2\Omega l^2/(l^2+m^2) & -\nu(l^2+m^2) \end{pmatrix} \; , \tag{29}$$

in which Ω is a rotation rate, α the constant shear of the mean flow, ν the coefficient of

viscosity, l the spanwise wavenumber, and m the vertical wavenumber (see Appendix) . With $\Omega = 0$ this matrix models the dynamical system of a streamwise roll perturbation in an unbounded constant shear boundary layer (Farrell and Ioannou 1993a). With $\Omega = 0$ this dynamical system is stable with decay rate $-\nu(l^2 + m^2)$ but with non-normality increasing with α so that it supports optimal transient growth increasing as α^2 and occurring at time $(\nu(l^2 + m^2))^{-1}$ implying that the variance grows as α^2 for constant viscosity. With the modification of including a spanwise oriented rotation rate Ω the decay of the least damped mode also decreases as α increases so that when $\alpha_c = 2\Omega + \nu^2(l^2 + m^2)^3/(2\Omega l^2)$ the matrix becomes unstable; the rotation rate Ω destabilizes the Reynolds matrix by coupling the streamwise and spanwise velocity components.

With this addition the Reynolds matrix provides a versatile example of the interplay of stability and non-normality in the vicinity of a stability boundary to which SSST generally adjusts jets. This matrix allows us to probe the mechanism producing power law behavior in strongly turbulent SSST equilibria such as the mid-latitude jet. When α is increased in the system with dynamical matrix $\mathbf{A}$ forced with constant variance white noise in each variable the variance maintained increases as α^2 while the variance in the equivalent normal system, in which the change in the eigenvalues is retained but the eigenvectors are assumed orthogonal, exhibits no power law behavior but only the $(\alpha - \alpha_c)^{-1}$ divergence in the immediate neighborhood of the stability boundary as shown in Fig. 5. The momentum flux also increases as α deviating from this power only in the immediate neighborhood of the critical shear.

Non-normailty induced power law behavior is generic in strongly turbulent equilibria in which the jet is adjusted to be near a stability boundary (Zhou and Stone 1993; Held and Larichev 1996; Barry et al. 2002; Zurita-Gotor 2007). While power law behavior is generic in strongly turbulent SSST equilibria the specific power depends on the stability parameter involved, the variable and the growth mechanism. This behavior can be understood by considering the growth of optimal perturbations which dominate the maintenance of variance in highly non-normal systems. The increase of the mean baroclinic and barotropic energy

generation rates

$$P_{em} = \int_0^1 -2\lambda^2 U^- \left\langle \overline{\psi_x^+ \psi^-} \right\rangle \, dy \tag{30a}$$

$$K_{em} = \int_0^1 \left[U^+ \left(\left\langle \overline{\psi_x^+ \psi_{yy}^+} + \overline{\psi_x^- \psi_{yy}^-} \right\rangle \right) + U^- \left(\left\langle \overline{\psi_x^+ \psi_{yy}^-} + \overline{\psi_x^- \psi_{yy}^+} \right\rangle \right) \right] dy \ , \tag{30b}$$

and of the quantity

$$vT = \left\langle \overline{\psi_x^+ \psi_{yy}^-} + \overline{\psi_x^- \psi_{yy}^+} \right\rangle \ , \tag{31}$$

which is proportional to the heat flux heat, with criticality of the equilibrated flow evaluated at the jet maxima $\xi = 4(U_1 - U_2)/(\beta L^2)$ is shown in Fig. 6. Both the energetic terms increase as ξ^4 in agreement with simulations which also show power law variation of the flux gradient relationship implying a higher order thermal diffusion with diffusivity increasing with the third power of the temperature gradient (Held and Larichev 1996; Zurita-Gotor 2007). The heat flux (at the center of the jet and its mean value) increase with criticality as ξ^3. At high criticality departures from the power law behavior shown in Fig. 6 result if the meridional average shear is used to calculate the criticality rather than the shear at the jet axis. The reason is that the shear becomes meridionally concentrated at high criticality. To show this the criticality calculated from the meridional average shear is shown as a function of the criticality calculated from the shear at the jet axis in Fig. 6

6. Destabilization and nonlinear equilibration of turbulent jets; sensitivity to static stability

A parameter of the baroclinic system that may vary with climate change is the static stability; in a warmer world troposphere static stability is expected to increase as a result of the decrease in the gradient of the saturated adiabat. This effect is generally accepted for the tropics and subtropics (Held 1982; Sarachik 1985; Xu and Emanuel 1989) and although the extent of the increase in the extratropics is less well established it is expected to also increase in midlatitudes (Juckes 2000; Frierson 1962). The opposite tendency is expected to characterize ice age climates.

The growth rate and structure of baroclinic waves are strongly influenced by static stability with the growth rate and the penetration depth scaling inversely with the buoyancy frequency (Valis 2006) so that it is of interest to add static stability to stochastic excitation and thermal gradient as parameters in our analysis.

Lower static stability implies higher Froude number as $\lambda^2 = (fL)^2/(NH)^2$. We show in Fig. 7 that the static stability serves as a bifurcation parameter analogous to the mean shear in its influence on SSST equilibria.

7. Quantization and Abrupt Jet Reorganization

As stochastic excitation is increased or mean shear is increased or static stability decreased equilibrium jets strengthen and adjust in structure to maintain a stable equilibrium. However, if the jet number is quantized, as is the case for the earth, eventually no stable jet equilibrium is possible at the extant wavenumber and the SSST system undergoes a bifurcation in which a new equilibrium is established typically at the next lowest wavenumber. This phenomenon has no counterpart in meridionally unbounded domains. This reorganization occurs abruptly as a parameter controlling jet amplitude is changed. This behavior has been observed to occur in model systems (Robinson 2006) and has been inferred to occur in the climate record (Fuhrer et al. 1999; Wunsch 2003; Alley et al. 1993). It provides a mechanism for producing abrupt changes in climate statistics by changing the source region of climate markers such as isotopes that are recorded in ice cores (Wunsch 2003). More fundamentally, because the axis of the polar jet is also an axis of concentration of surface stress, the abrupt displacement of the polar jet could change the climate itself by influencing the ventilation of the deep ocean, (Toggweiler et al. 2006). An example of bifurcation from a wavenumber 3 to a wavenumber 2 jet is shown in Fig. 8. In this example we have chosen to induce bifurcation by increasing the Froude number corresponding physically to decreasing the static stability. At $\lambda^2 = 1.2$ there is an abrupt transition from a meridional wavenumber 3 jet to a meridional wavenumber 2 jet for thermal forcing $\Delta T = 30$ K/(10^4km) and stochastic excitation of $f = 0.49$ mWkg^{-1} per mode.

8. Discussion

a. Relation between SSST equilibria and the barotropic governor

It was noticed by James (1987) that jets in GCM simulations tend to equilibrate by modifying the barotropic shear and that substantially greater baroclinic shear can be maintained in these horizontally sheared flows than would be compatible with stability in a horizontally homogeneous flow. This phenomenon, called the barotropic governor, was confirmed by stability analyses and it implied that baroclinic adjustment process is accomplished in part independently of heat transport and changes in the vertical shear (Lindzen 1993). The SSST equilibria provide insight into the mechanism underlying the barotropic governor by showing that a barotropic governor stabilized state is an attracting equilibrium state of the ensemble mean eddy/mean flow coupled system. This mechanism of stabilization by confinement due to horizontal shear which we have seen in the two layer model was analyzed by Ioannou and Lindzen (1986) and Roe and Lindzen (1996).

b. Relation between SSST equilibria and baroclinic adjustment

Baroclinic adjustment was originally invoked to explain the tendency of baroclinic jets to be associated with a relatively constant temperature gradient in models and in observations (Stone 1978; Stone and Miller 1980). Baroclinic adjustment is important as a concept because of the insight it offers into the nature of baroclinic turbulence. It is also important as the theoretical underpinning for the concept of compensation in baroclinic turbulence which has implications for climate dynamics. The idea of baroclinic compensation is that since baroclinic turbulence maintains a relatively constant temperature gradient in mid and high latitudes the influence of any change in alternative heat transport mechanisms such as ocean heat transport is diminished: the baroclinic transport adjusts up or down to compensate for any variation in these transport mechanisms so their variation can not substantially change the climate. Baroclinic adjustment has been extensively studied and two main ideas have emerged: adjustment due to modal instabilities themselves producing the heat flux when the stability boundary is crossed and these modal instabilities then adjust the system to a

stability boundary (Stone 1978; Cehelsky and Tung 1991; Gutowski et al. 1989; Lindzen and Farrell 1980; Lindzen 1993); and high order turbulent diffusion due to structural changes in baroclinic eddies producing rapid increase in heat transport coincident with the stability boundary but not causally related to unstable growth itself (Pavan and Held 1996; Held and Larichev 1996). We have seen that SSST equilibria approach a stability boundary when the turbulence is sufficiently strong and so these equilibria provide a natural explanation for the phenomenon of baroclinic adjustment. This explanation unites the previous interpretations in the following sense: the stability boundary is important but not, as in the original baroclinic adjustment interpretations, because growth occurs when this boundary is exceeded but rather because it is an equilibrium state of the SSST coupled meanflow/turbulence system. Turbulent transport is important because it is the spectrum of waves not just the instabilities that produce the transport but the equilibrium flux/gradient relationship can not be understood from homogeneous turbulence closure arguments because the transport at equilibrium is essentially related to the inhomogeneity of the equilibrium states and particularly to the organization of the horizontal shear.

9. Conclusions

Steady stable coherent large scale mean zonal jets emerge spontaneously from baroclinic turbulence in the absence of jet scale forcing; examples include the Jovian banded winds and the Earth's polar front jet . The primary physical mechanism maintaining these jets is turbulent eddy fluxes which have been systematically organized by the jet to support the jet structure. This phenomenon arises from an ubiquitous instability of turbulent fluids to jet formation which occurs because turbulent eddies are always available to be organized by an appropriately configured perturbation zonal jet to produce a flux proportional to jet amplitude. Because this local upgradient flux is proportional to jet amplitude it results at first in exponential jet growth rate. This is a new mechanism for destabilizing turbulent flows which is essentially emergent from the interaction between the mean state and its turbulence. In this work we have provided a detailed dynamical explanation for the systematic mutual organization of the jet and the turbulent eddy fluxes required to produce this instability. A key ingredient of this theory is stochastic turbulence modelling which provides an analytic solution for the eddy covariance in statistical equilibrium with the jet so that this feedback between the jet and the turbulence can be analyzed in detail. The primary analytical tool of SSST is the coupled dynamical system consisting of the evolution equation for the eddy fluxes obtained from a statistical equilibrium stochastic turbulence model together with the evolution equation for the zonal jet. This nonlinear coupled set of equations exhibits robust and relatively simple behavior. Using this model we find that the state of thermal wind balance with a constant temperature gradient in a doubly periodic beta plane channel is a stationary state of the coupled system for baroclinically stable states but that this stationary state is exponentially unstable to zonal jet perturbations if the turbulence is sufficiently strong and that these zonal perturbations evolve into jets that grow and adjust in structure until reaching finite amplitude equilibrium. If a baroclinically unstable mean shear is relaxed to then the equilibration is a function of both the thermal gradient and the stochastic excitation but equilibria are still found.

With weak excitation the equilibrated jets are sinusoidal and nearly barotropic. There may be a number of unstable meridional jet wavenumbers each leading to an equilibrated

state. If evolved from an unbiased initial condition the wavenumber of a weakly forced jet would be that of the most unstable eigenmode of the linearized SSST system and the amplitude that obtained from balance between the weakly nonlinearly modified upgradient eddy momentum flux and dissipation. But as the stochastic excitation, or another stability related parameter such as the static stability, changes so as to tend to destabilizing the jet its structure becomes baroclinic and evolves in a characteristic progression that contrives to maintain the jet equilibria near a modal eddy stability boundary despite the increase in jet amplitude arising from the increasing excitation. The eastward jet contracts and becomes increasingly baroclinic. This contraction of meridional scale augments the effective beta as does an arbitrary vertical shear so the eastward jet shear may become quite large. This mechanism stabilizing the baroclinic mode in eastward shear may be viewed as a manifestation of the barotropic governor (Ioannou and Lindzen 1986; James 1987; Lindzen 1993). No such stabilization of the westward jet is possible so the vertical shear is maintained small in the westward jet to prevent baroclinic eddy mode destabilization while the meridional scale expands to approach the Rayleigh-Kuo condition for barotropic modal stability which approximates the Rhines scale. Consequently the equilibrium jet structure exhibits pronounced asymmetry with the eastward jet being sharper than the westward jet and of the three space scales in the jet structure problem the Rhines scale emerges as the primary meridional structure scale.

Dissipation and quantization of both meridional and zonal wavenumbers often results in marginally stable states that in some degree satisfy either or both of the Charney-Stern and Rayleigh-Kuo conditions. This is no contradiction because these conditions are necessary and not sufficient conditions and in any case apply strictly only to unbounded flows without dissipation. It is important to keep in mind that the fact that an observed jet does not satisfy one or both of these necessary conditions does not imply that the jet is unstable.

Adjustment of jets to marginal stability can take place in many ways including reducing the vertical shear, increasing the horizontal shear, and in the primitive equations modifying the static stability. As all of these mechanisms are available, only knowing that the system is adjusted to a state of marginal stability, while useful as a diagnostic, does not constitute a predictive theory for jet structure. One great innovative advantage of SSST is that it

transcends this ambiguity by the crucial additional requirement of equilibrium between the turbulent fluxes and the jet which identifies in the space of all marginal equilibria that one which is consistent and therefore is the physically relevant one.

We show that adjustment to stable but highly amplifying states with power law behavior for flux/gradient relations is characteristic of the equilibria that arise. Analogous behavior often arises when a feedback controller is imposed to stabilize a multidimensional unstable mechanical or electronic system (Zhou and Doyle 1998). We have shown that the state of high non-normality together with marginal stability is inherent because turbulence maintains flow stability with a naturally occurring feedback controller.

In the presence of meridional quantization such as that enforced by finite planetary radius an abrupt reorganization of jet structure occurs as stochastic forcing or another parameter controlling jet amplitude increases. This reorganization occurs as the increasing westward jet amplitude forces sufficient violation of the Rayleigh-Kuo condition to produce an incipient instability for the dissipation and spatial confinement of the model. At this point the jet reorganizes to the next lower allowed meridional wavenumber and the process continues.

This abrupt reorganization of jet structure as a function of slow parameter change is an example of a fundamental process in jet dynamics with important climate connections. Discontinuous reorganization of eddy driven jets can alter both climate statistics (Fuhrer et al. 1999; Wunsch 2003) and the climate itself (Toggweiler et al. 2006). Abrupt change of climate and climate statistics is common in the climate record (Alley et al. 1993) but mechanisms for producing abrupt transitions have been difficult to find. Storm track reorganization is an alternative and perhaps complementary mechanism to reorganization of thermohaline circulations (Weaver et al. 1991; Kaspi et al. 2004) and sea-ice switches (Gildor and Tziperman 2003) for explaining the record of abrupt climate change.

This work provides a detailed physical theory for the emergence of jet structure and structural transition in baroclinic turbulence. For reasons of theoretical clarity we have chosen to concentrate on the case of jets for which the meridional scale is not externally influenced. However, the meridional structure of the Earth's subtropical jet is forced and this jet would exist even in the absence of eddies (Held and Hou 1980) while the polar front jet is essentially eddy maintained. Extension of this work to address jet structure and

transition when a large scale meridional structure is imposed will be the subject of future work.

Acknowledgments.

This work was supported by NSF ATM-0123389.

APPENDIX

The Reynolds matrix

The perturbation equations governing the evolution of the (x, y, z) perturbation velocities (u, v, w) and pressure (p) of the harmonic form:

$$[u, v, w, p] = [\hat{u}(t), \hat{v}(t), \hat{w}(t), \hat{p}(t)]e^{i(ly+mz)} \ , \tag{A1}$$

in an unbounded constant shear flow $\alpha z \ \vec{i}$ in a frame rotating in the $-\Omega \ \vec{j}$ direction are:

$$\frac{d\hat{u}}{dt} = -(\alpha - 2\Omega)\hat{w} - \nu(l^2 + m^2)\hat{u} \tag{A2a}$$

$$\frac{d\hat{v}}{dt} = -il\hat{p} - \nu(l^2 + m^2)\hat{v} \tag{A2b}$$

$$\frac{d\hat{w}}{dt} = -im\hat{p} - 2\Omega\hat{u} - \nu(l^2 + m^2)\hat{w} \ . \tag{A2c}$$

These equations describe the evolution of x independent perturbations. These perturbations excite roll circulations in the (y, z) plane associated with zonal (x) streaks (Farrell and Ioannou 1993a).

Using the continuity equation we obtain

$$\hat{p} = \frac{2im\Omega}{l^2 + m^2}\hat{u} \ , \tag{A3}$$

eliminating the pressure from the vertical (z) velocity equation we obtain the dynamical system

$$\frac{d\hat{u}}{dt} = -\nu(l^2 + m^2)\hat{u} - (\alpha - 2\Omega)\hat{w} \tag{A4a}$$

$$\frac{d\hat{w}}{dt} = -\frac{2l^2\Omega}{l^2 + m^2}\hat{u} - \nu(l^2 + m^2)\hat{w} \ . \tag{A4b}$$

For constant parameters the perturbation dynamics are governed by the matrix:

$$\mathbf{A} \;=\; \begin{pmatrix} -\nu(l^2+m^2) & -(\alpha-2\Omega) \\ -2\Omega l^2/(l^2+m^2) & -\nu(l^2+m^2) \end{pmatrix} \;. \tag{A5}$$

The dynamics are stable if the shear of the mean flow is smaller than $\alpha_c = 2\Omega + \nu^2(l^2 + m^2)^3/(2\Omega l^2)$.

When the dynamics are stable the ensemble mean energy density for unit mass density $< E >= \langle \hat{u}^2 + \hat{v}^2 + \hat{w}^2 \rangle /4$ maintained under white stochastic excitation with unit covariance is

$$\langle E \rangle = \frac{1}{4}\left(C_{11} + \frac{l^2+m^2}{l^2} C_{22} \right) \;, \tag{A6}$$

where the perturbation covariance matrix $\mathbf{C} = \left\langle [\hat{u}, \hat{w}][\hat{u}, \hat{w}]^\dagger \right\rangle$ solves the Lyapunov equation

$$\mathbf{AC} + \mathbf{CA}^\dagger = -\mathbf{I} \;. \tag{A7}$$

The solution is

$$C_{11} = \frac{2\nu^2(l^2+m^2)^3 - 2fl^2(\alpha-2\Omega) + (\alpha-2\Omega)^2(l^2+m^2)}{8\nu^3(l^2+m^2)^4} E_n \tag{A8a}$$

$$C_{22} = \frac{\nu^2(l^2+m^2)^4 - \Omega l^2(\alpha-2\Omega)(l^2+m^2) + \Omega^2 l^4}{4\nu^3(l^2+m^2)^5} E_n \tag{A8b}$$

$$C_{12} = C_{21} = -\frac{\alpha(l^2+m^2) + 2\Omega l^2}{8\nu^2(l^2+m^2)^3} E_n \;, \tag{A8c}$$

where

$$E_n = \frac{\nu(l^2+m^2)^2}{\nu^2(l^2+m^2)^3 - 2\Omega l^2(\alpha - 2f))} \tag{A9}$$

is the total variance maintained by the equivalent normal system

$$\mathbf{A}_n \;=\; \begin{pmatrix} -\nu(l^2+m^2) + \sqrt{2\Omega l^2(\alpha-2\Omega)}/\sqrt{l^2+m^2} & 0 \\ 0 & -\nu(l^2+m^2) - \sqrt{2\Omega l^2(\alpha-2\Omega)}/\sqrt{l^2+m^2} \end{pmatrix} \;. \tag{A10}$$

that has the same eigenvalues as (A5).

As the shear α increases the equivalent normal total variance E_n increases only in the

neighborhood of the critical shear α_c where the system becomes unstable (see Fig. 5). The non-normality of the Reynolds matrix is responsible for the power law behavior of the maintained variance and the flux. Except in the immediate neighborhood of α_c, as α increases $< \hat{u}^2 >= C_{11}$ increases as α^2 , $< \hat{w}^2 >= l^2 < \hat{v}^2 > /m^2 = C_{22}$ increases as α and $\langle \overline{uw} \rangle = C_{12}/2$ increases also as α.

REFERENCES

Alley, R. B., et al., 1993: Abrupt increase in Greenland snow accumulation at the end of the Younger Dryas event. *nat*, **362**, 527–529, doi:10.1038/362527a0.

Barry, L., G. C. Craig, and J. Thurbun, 2002: Poleward heat transport by the atmospheric heat engine. *Nature*, **415**, 774–777.

Bobba, K. M., B. Bamieh, and J. C. Doyle, 2007: Highly optimized transitions to turbulence. *Phys. Rev. Lett.*, **13**, 123–456.

Cehelsky, P. and K. Tung, 1991: Nonlinear baroclinic adjustment. *JAS*, **48**, 1930–1947.

Cho, J. Y.-K. and L. M. Polvani, 1996: The morphogenesis of bands and zonal winds in the atmospheres on the giant outer planets. *Science*, **273**, 335–337.

DelSole, T., 1996: Can quasigeostrophic turbulence be modeled stochastically? *J. Atmos. Sci.*, **53**, 1617–1633.

DelSole, T., 1999: Stochastic models of shear-flow turbulence with enstrophy transfer to subgrid scales. *J. Atmos. Sci.*, **56**, 3692–3703.

DelSole, T., 2004a: The necessity of instantaneous optimals in stationary turbulence. *J. Atmos. Sci.*, **61**, 1086–1091.

DelSole, T., 2004b: Stochastic models of quasigeostrophic turbulence. *Surveys in Geophysics*, **25**, 107–194.

DelSole, T. and B. F. Farrell, 1995: A stochastically excited linear system as a model for quasigeostrophic turbulence: Analytic results for one- and two-layer fluids. *J. Atmos. Sci.*, **52**, 2531–2547.

DelSole, T. and B. F. Farrell, 1996: The quasi-linear equilibration of a thermally mantained stochastically excited jet in a quasigeostrophic model. *J. Atmos. Sci.*, **53 (13)**, 1781–1797.

Dowling, T. E., 1994: Successes and failures of shallow-water interpreations of voyager wind data. **4**, 213–225.

Farrell, B. F., 1982: The initial growth of disturbances in a baroclinic flow. *J. Atmos. Sci.*, **39**, 1663–1686.

Farrell, B. F., 1985: Transient growth of damped baroclinic waves. *J. Atmos. Sci.*, **42**, 2718–2727.

Farrell, B. F., 1989: Optimal excitation of baroclinic waves. *J. Atmos. Sci.*, **46**, 1193–1206.

Farrell, B. F. and P. J. Ioannou, 1993a: Optimal excitation of three dimensional perturbations in viscous constant shear flow. *Physics of Fluids*, **5**, 1390–1400.

Farrell, B. F. and P. J. Ioannou, 1993b: Perturbation growth in shear flow exhibits universality. *Physics of Fluids*, **5**, 2298.

Farrell, B. F. and P. J. Ioannou, 1993c: Stochastic dynamics of baroclinic waves. *J. Atmos. Sci.*, **50**, 4044–4057.

Farrell, B. F. and P. J. Ioannou, 1994: A theory for the statistical equilibrium energy spectrum and heat flux produced by transient baroclinic waves. *J. Atmos. Sci.*, **51**, 2685–2698.

Farrell, B. F. and P. J. Ioannou, 1995: Stochastic dynamics of the midlatitude atmospheric jet. *J. Atmos. Sci.*, **52**, 1642–1656.

Farrell, B. F. and P. J. Ioannou, 1996: Generalized stability. Part I: Autonomous operators. *J. Atmos. Sci.*, **53**, 2025–2040.

Farrell, B. F. and P. J. Ioannou, 2003: Structural stability of turbulent jets. *J. Atmos. Sci.*, **60 (17)**, 2101–2118.

Farrell, B. F. and P. J. Ioannou, 2007: Structure and spacing of jets in barotropic turbulence. *J. Atmos. Sci.*, **63**.

Frierson, D. M. W., 1962: Robust increases in midlatitude static stability in simulations of global warming. *Geophys. Res. Lett.*, **33**, L24 816, doi: 10.1029/2006GL027 504.

Fuhrer, K., E. W. Wolff, and S. J. Johenses, 1999: Timescales for dust variability in the Greenland Ice Core Project (GRIP) ice core in the last 100,000 years. *JGR*, **104**, 31,043–31,052.

Galperin, B., H. Nakano, H.-P. Huang, and S. Sukoriansky, 2004: The ubiquitous zonal jets in the atmospheres of giant planets and earth's oceans. *Geophys. Res. Lett.*, **31**, 13 303–13 308.

Gildor, H. and E. Tziperman, 2003: Sea-ice switches and abrupt climate change. *Phil. Trans. R. Soc. Lond.*, **361**, 1935–1944.

Gutowski, W. J., 1985: Baroclinic adjustment and midlatitutde temperature profiles. *J. Atmos. Sci.*, **42**, 1733–1745.

Gutowski, W. J., L. E. Branscome, and D. A. Stewart, 1989: Mean flow adjustment during life cycles of baroclinic waves. *JAS*, **46**, 1724–1737.

Hall, N. M. J. and P. D. Sardeshmukh, 1998: Is the time-mean northern hemisphere flow baroclinically unstable? *J. Atmos. Sci.*, **55**, 41–56.

Held, I. M., 1978: On the Vertical Scale of an Unstable Baroclinic Wave and Its Importance for Eddy Heat Flux Parameterizations . *J. Atmos. Sci.*, **35**, 572–576.

Held, I. M., 1982: On the height of the tropopause and the static stability of the troposphere. *J. Atmos. Sci.*, **39**, 412–417.

Held, I. M., 1999: The macroturbulence of the troposphere. *Tellus*, **51**, 59–70.

Held, I. M. and A. Y. Hou, 1980: Nonlinear Axially Symmetric Circulations in a Nearly Inviscid Atmosphere. *J. Atmos. Sci.*, **37**, 515–533.

Held, I. M. and V. D. Larichev, 1996: A scaling theory for horizontally homogeneous, baroclinically unstable flow on a beta plane. *JAS*, **53**, 946–952.

Huang, H.-P. and W. A. Robinson, 1998: Two-dimensional turbulence and persistent zonal jets in a global barotropic model. *J. Atmos. Sci.*, **55**, 611–632.

Ingersoll, A. P., 1990: Atmospheric dynamics of the outer planets. *Science*, **248**, 308–315.

Ioannou, P. J. and R. S. Lindzen, 1986: Baroclinic instability in the presence of barotropic jets. *J. Atmos. Sci.*, **43**, 2999–3014.

James, I. N., 1987: Suppression of Baroclinic Instability in Horizontally Sheared Flows. *Journal of Atmospheric Sciences*, **44**, 3710–3720.

Jeffreys, H., 1933: The function of cyclones in the general circulation. *Proces.-Verbaux de l'Association de Meteorologie*, UGGI (Lisbon), Part II, 219–230.

Juckes, M. N., 2000: The static stability of the midlatitude troposphere: The relevance of moisture. Vol. 57, 3050–3057.

Kaspi, Y. H., R. Sayag, and E. Tziperman, 2004: A 'triple sea-ice state' mechanism for the abrupt warming and synchronous ice sheet collapses during Heinrich events. *Paleoceanography*, **19**, PA3004.

Koo, S., A. W. Robertson, and M. Ghil, 2002: Multiple regimes and low frequency oscillations in the southern hemisphere's zonal mean flow. *J. Geophys. Res.*, **107**, 4596–4609.

Krishnamurti, R. and L. N. Howard, 1981: Large-scale flow generation in turbulent convection. *Proc. Natl. Acad. Sci. U.S.A.*, **78**, 1981–1985.

Lee, S., 2005: Baroclinic multiple jets on the sphere. *J. Atmos. Sci.*, **62**, 2484–2498.

Lee, S. and H. Kim, 2003: The Dynamical Relationship between Subtropical and Eddy-Driven Jets. *J. Atmos. Sci.*, **60**, 1490–1503.

Li, C., D. S. Battisti, D. P. Schrag, and E. Tziperman, 2005: Abrupt climate shifts in greenland due to displacements of the sea ice edge. *Geophys. Res. Lett.*, **32**, L19 702, doi:10.1029/2005GL023 492.

Lindzen, R. S., 1993: Baroclinic neutrality and the tropopaus. *J. Atmos. Sci.*, **50**, 1148–1151.

Lindzen, R. S. and B. F. Farrell, 1980: The role of polar regions in global climate, and a new parameterization of global heat transport. *MWR*, **108**, 2064–2079.

Manfroi, A. J. and W. R. Young, 1999: Slow evolution of zonal jets on the beta plane. *J. Atmos. Sci.*, **56**, 784–800.

Newman, M., P. D. Sardeshmukh, and C. Penland, 1997: Stochastic forcing of the wintertime extratropical flow. *J. Atmos. Sci.*, **54**, 435–455.

Nozawa, T. and Y. Yoden, 1997: Formation of zonal band structure in forced tw0-dimensional turbulence on a rotating sphere. *Physics of Fluids*, **9**, 2081–2093.

Panetta, R. L., 1993: Zonal jets in wide baroclinically unstable regions: persistence and scale selection. *J. Atmos. Sci.*, **50**, 2073–2106.

Pavan, P. and I. M. Held, 1996: The diffusive approximation for eddy fluxes in baroclinically unstable jets. *JAS*, **53**, 1262–1272.

Read, P. L., Y. H. Yamazaki, S. R. Lewis, P. D. Williams, K. Miki-Yamazaki, J. Sommeria, H. Didelle, and A. Fincham, 2004: Jupiter's and saturn's convectively driven banded jets in the laboratory. *Geophys. Res. Lett.*, **87**, 1961–1967.

Read, P. L., Y. H. Yamazaki, S. R. Lewis, P. D. Williams, R. Wordsworth, and K. Miki-Yamazaki, 2007: Dynamics of convectively driven banded jets in the laboratory. *J. Atmos. Sci.*, **64**, 4031–4052.

Rhines, P. B., 1975: Waves and turbulence on a beta plane. *J. Fluid Mech.*, **69**, 417–433.

Robinson, W. A., 2006: On the Self-Maintenance of Midlatitude Jets. *Journal of Atmospheric Sciences*, **63**, 2109–2122.

Roe, H. H. and R. S. Lindzen, 1996: Baroclinic adjustment in a two-level model with barotropic shear. *J. Atmos. Sci.*, **53**, 2749–2754.

Sarachik, E. S., 1985: A simple theory for the vertical structure of the tropical atmosphere. *PAG*, **123**, 261–271.

Sardeshmukh, P. D. and P. Sura, 2007: Multiscale impacts of variable heating in climate. *J. Climate*, **20**, 5677–5695.

Schneider, T. and C. C. Walker, 2006: Self-organization of atmospheric macroturbulence into critical states of weak nonlinear eddy-eddy interactions. *J. Atmos. Sci.*, **63**, 1569–1586.

Stone, P. H., 1978: Baroclinic adjustment. *J. Atmos. Sci.*, **35**, 561–571.

Stone, P. H. and L. Branscome, 1992: Diabatically forced, nearly inviscid eddy regimes. *J. Atmos. Sci.*, **49**, 355–367.

Stone, P. H. and D. A. Miller, 1980: Empirical relations between seasonal changes in meridional temperature gradients and meridional fluxes of heat. *J. Atmos. Sci.*, **37**, 1708–1721.

Toggweiler, J. R., J. L. Russell, and S. R. Carson, 2006: Midlatitude westerlies, atmospheric CO_2, and climate change during the ice ages. *Paleoceanography*, **21**, A2005+.

Valis, G. K., 2006: *Atmospheric and Oceanic Fluid Dynamics*. Cambridge University Press, Cambridge England.

Vallis, G. K. and M. E. Maltrud, 1993: Generation of mean flows and jets on a beta plane and over topography. *J. Phys. Oceanogr.*, **23**, 1346–1362.

Vasavada, A. R. and A. P. Showman, 2005: The growth of gravity-capillary waves in a coupled shear flow. *Rep. Prog. Phys.*, **68**, 1935–1996.

Weaver, A. J., E. S. Sarachik, and J. Marotze, 1991: Freshwater flux forcing of decadal and interdecadal oceanic variability. *nat*, **353**, 836–838.

Welch, W. T. and K.-K. Tung, 1998: Nonlinear baroclinic adjustment and wavenumber selection in a simple case. *J. Atmos. Sci.*, **55**, 1285–1302.

Whitaker, J. S. and P. D. Sardeshmukh, 1998: A linear theory of extratropical synoptic eddy statistics. *J. Atmos. Sci.*, **55**, 237–258.

Williams, G. P., 1979: Planetary circulations: 2. the jovian quasi-geostrophic regime. *J. Atmos. Sci.*, **36**, 932 – 968.

Williams, G. P., 2003: Jet sets. *J. Met. Soc. Jap.*, **81**, 439–476.

Wunsch, C., 2003: Greenland-Antarctic phase relations and millennial time-scale climate fluctuations in the Greenland ice-cores. *Quaternary Science Reviews*, **22**, 1631–1646.

Xu, K.-M. and K. A. Emanuel, 1989: Is the tropical atmosphere conditionally unstable? *MWR*, **117**, 1471–1479.

Zhang, Y. and I. M. Held, 1999: ä linear stochastic model of a gcm's midlatitude storm tracks. *J. Atmos. Sci.*, **56**, 3416–3435.

Zhou, K. and J. C. Doyle, 1998: *Essentials of Robust Control*. Prentice Hall.

Zhou, S. and P. H. Stone, 1993: The role of large-scale eddies in the climate equilibrium. Part I: Fixed static stability. *J. Climate*, **6**, 985–1001.

Zurita-Gotor, P., 2007: The relation between baroclinic adjustment and turbulent diffusion in the two-layer model. *J. Atmos. Sci.*, **64**, 1284–1300.

Zurita-Gotor, P. and R. S. Lindzen, 2004a: Baroclinic equilibration and the maintenance of the momentum balance. Part I: A barotropic analog. *J. Atmos. Sci.*, **61**, 1469–1482.

Zurita-Gotor, P. and R. S. Lindzen, 2004b: Baroclinic equilibration and the maintenance of the momentum balance. Part II: 3 D results. *J. Atmos. Sci.*, **61**, 1485–1501.

List of Figures

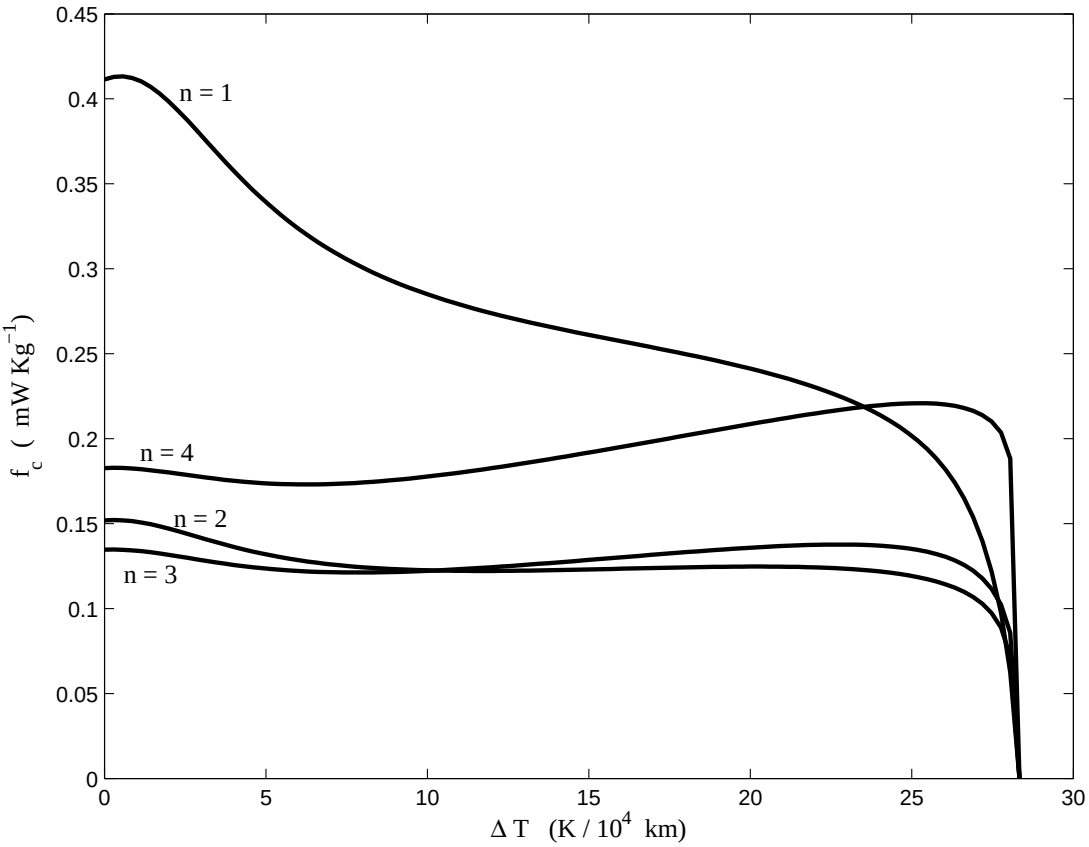

FIG. 1. The critical value of forcing f_c (mW kg^{-1}) required to structurally destabilize the imposed mean flow that maintains a ΔT $(K/(10^4\ km))$ temperature difference. The different curves correspond to the critical forcing required for the emergence of a zonal flow with meridional wavenumber $n = 1, .., 4$. The eddy field comprises global zonal wavenumbers 1-14.

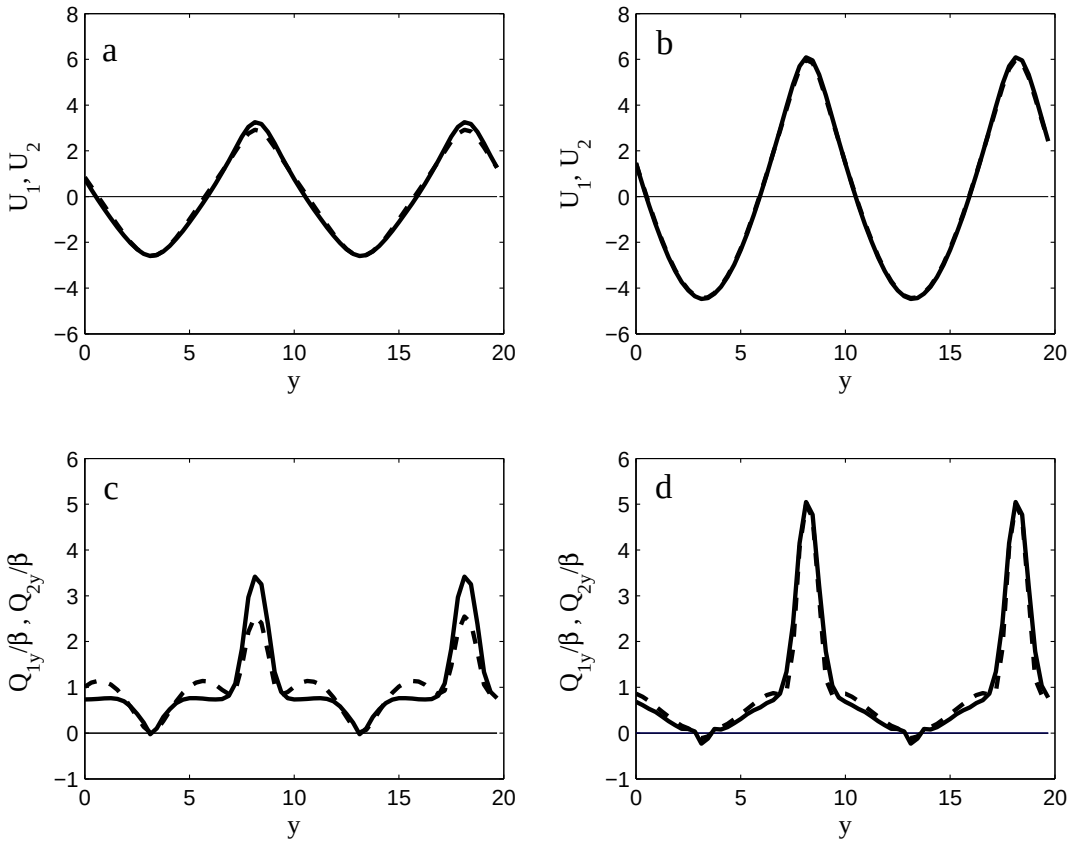

FIG. 2. Meridional structure of the equilibrium upper layer (continuous line) and lower layer (dashed line) mean flows maintained in a channel with no mean thermal forcing. Equilibria for two levels of stochastic excitation f are shown. In (a) the stochastic excitation is $f = 5.83$ mWkg^{-1} per zonal wavenumber. In (b) the stochastic excitation is $f = 58.3$ mWkg^{-1} per zonal wavenumber. In c, d are shown the corresponding mean potential vorticity gradients of the upper and lower layer flows. The non-normality of the equilibrium flows has increased from 53.9 for the flows in (a) to 155 for the flows in (b). The eddy field comprises global zonal wavenumbers 1-14. The eddy damping parameters are $r_2 = 1/5$ d^{-1} and $r_R = 1/15$ d^{-1} and the damping rate of the mean is $\overline{r}_2 = 1/5$ d^{-1} and the mean cooling is $\overline{r}_R = 1/15$ d^{-1} .

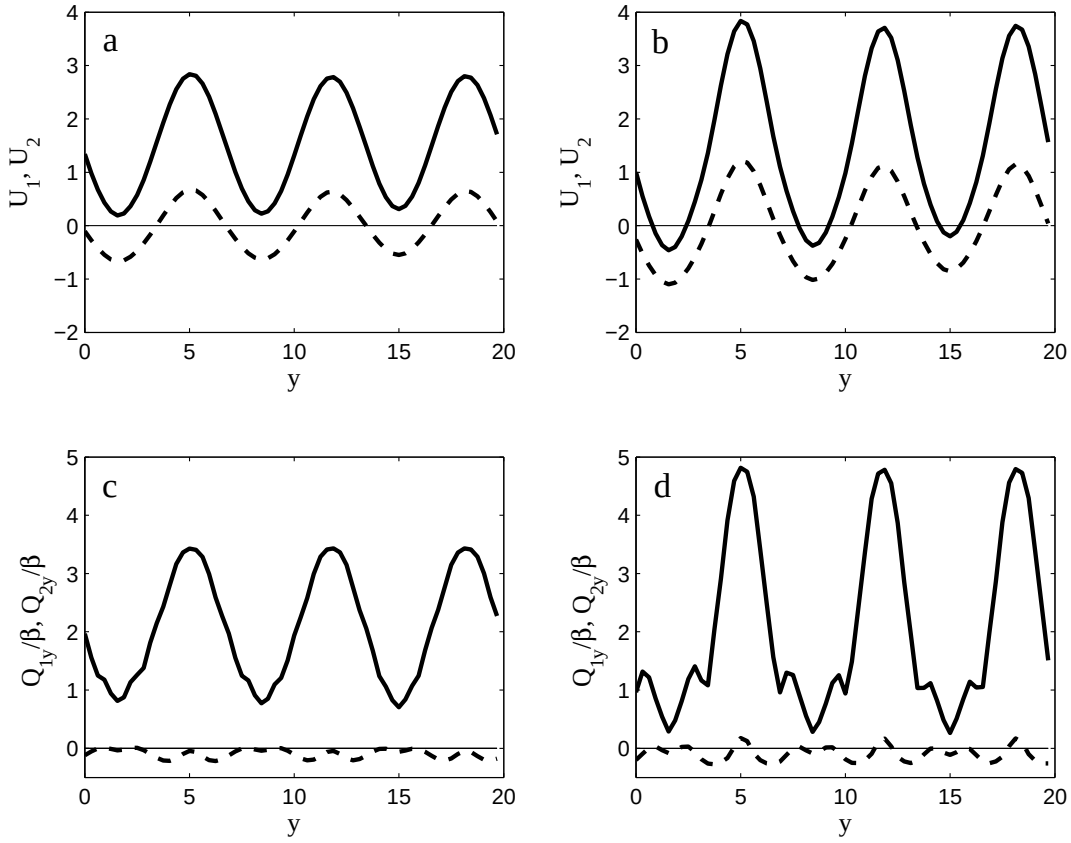

FIG. 3. Meridional structure of the equilibrium upper layer (continuous line) and lower layer (dashed line) mean flows maintained in a channel with mean thermal forcing $\Delta T = 30$ K/(10^4 km). Equilibria for two levels of stochastic excitation f are shown. In (a) the stochastic excitation is $f = 0.48$ mWkg^{-1} per zonal wavenumber. In (b) the stochastic excitation is $f = 1.34$ mWkg^{-1} per zonal wavenumber. In c, d are shown the corresponding mean potential vorticity gradients of the upper and lower layer flows. The non-normality of the equilibrium flows has increased from 26.7 for the flows in (a) to 53 for the flows in (b). The eddy field comprises global zonal wavenumbers 1-14. The eddy damping parameters are $r_2 = 1/5$ d^{-1}, $r_R = 1/15$ d^{-1}, $r_{eff} = 1/20$ d^{-1} and the damping rate of the mean is $\overline{r}_2 = 1/5$ d^{-1} and the mean cooling is $\overline{r}_R = 1/15$ d^{-1} .

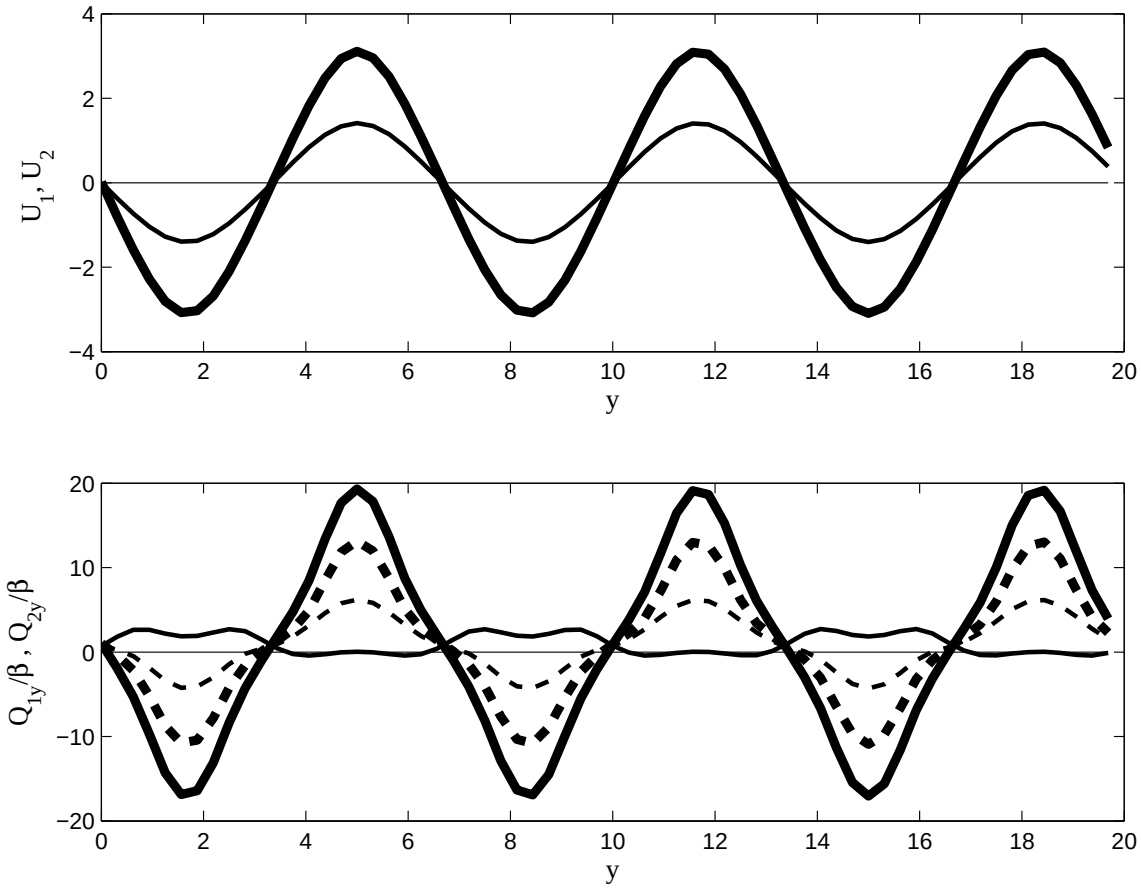

FIG. 4. Meridional structure of the equilibrium upper layer (continuous thick line) and lower layer (continuous line) mean flows maintained in a channel with no mean thermal forcing. The parameters have been chosen in order to reproduce Jovian conditions. Both layers are equally damped at a rate $r_1 = r_2 = 1$ d^{-1}, eddy cooling of $r_R = 1/15$ d^{-1}, and dissipation of the mean $\overline{r}_1 = \overline{r}_2 = 1/250$ d^{-1} with stochastic excitation of only the upper layer at level $f = 0.972$ mWkg^{-1}. The other parameters are $\lambda^2 = 1$ and beta is 1/5 of the terrestrial β. In (b) are shown the corresponding mean potential vorticity gradients measured in units of β of the upper (solid thick line) and lower (dashed thick line) layer layer flows . Also shown are the corresponding barotropic potential vorticity gradients (solid and dashed lines). Although the potential vorticity strongly violates the Rayleigh-Kuo stability condition the flow is stable.

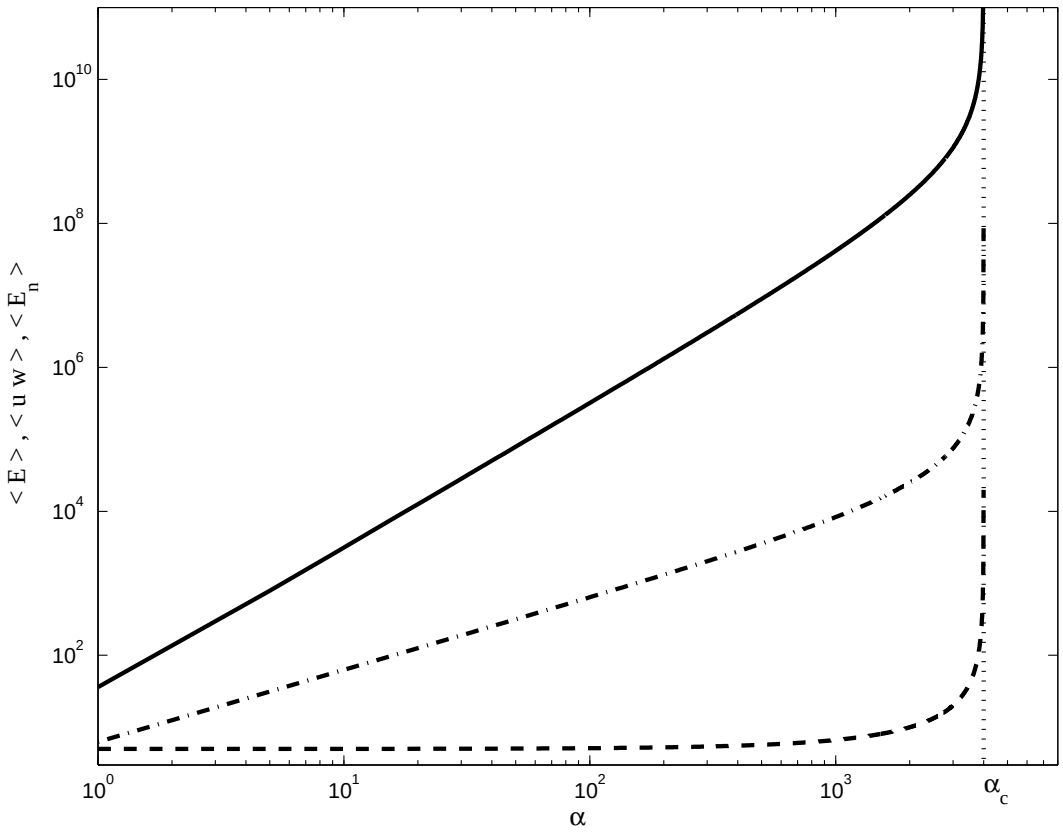

FIG. 5. For the Reynolds example system shown are: the ensemble mean energy $< E >$ as a function of the shear α for rotation rate $\Omega = 10^{-5}$, viscosity $\nu = 0.1$ and perturbation wavenumbers $l = m = 1$. The critical shear at which the matrix becomes unstable is $\alpha_c = 4000$. The variance increases as α^2 deviating from this power law behavior only for shears very close to α_c. The dash-dot curve shows similar behavior for the momentum flux $< \overline{uw} >$ which can be seen to vary as α. The dashed curve shows the variance, $< E_n >$, maintained by the equivalent normal system with the same decay rate as $\mathbf{A}$; this variance is almost constant increasing only for shears close to α_c. .

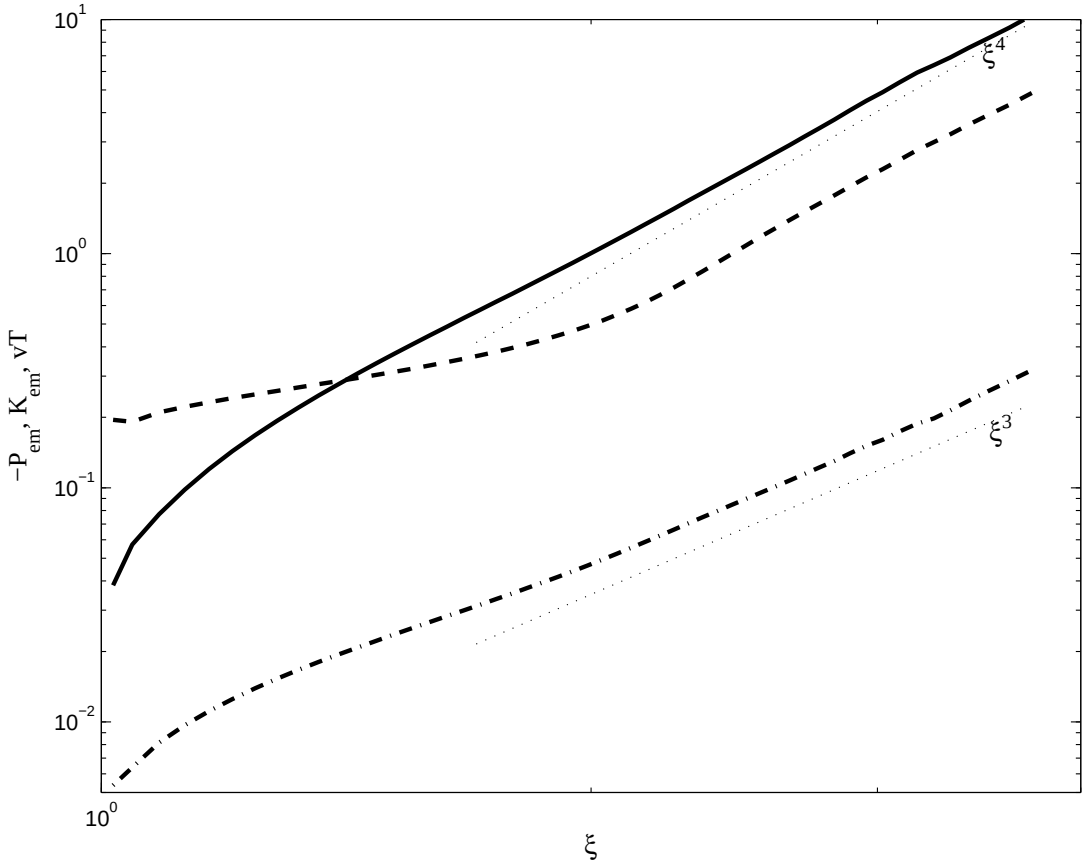

FIG. 6. For the equilibrated jets shown are: the mean eddy baroclinic energy generation rate $-P_{em}$ (solid line), the mean eddy barotropic energy generation rate K_{em} (dashed line) and ~~of~~ the heat flux ~~vT~~ at the center of the jet (dash-dot line) as a function of the criticality parameter $\xi = \frac{4(U_1-U_2)}{\beta L_2}$ evaluated at the jet maximum. The eddy generation rates increase as ξ^4 (indicated with the dotted line) and the heat flux increases as ξ^3 (indicated with the dotted line). The mean heat flux also has the same power law behavior. The stochastic excitation is $f = 0.24$ mWkg^{-1} per mode. The eddy field comprises global zonal wavenumbers 1-14. The eddy damping parameters are $r_2 = 1/5$ d^{-1}, $r_R = 1/15$ d^{-1}, $r_{eff} = 1/20$ d^{-1} and the damping rate of the mean is $\overline{r}_2 = 1/5$ d^{-1} and the mean cooling is $\overline{r}_R = 1/15$ d^{-1} .

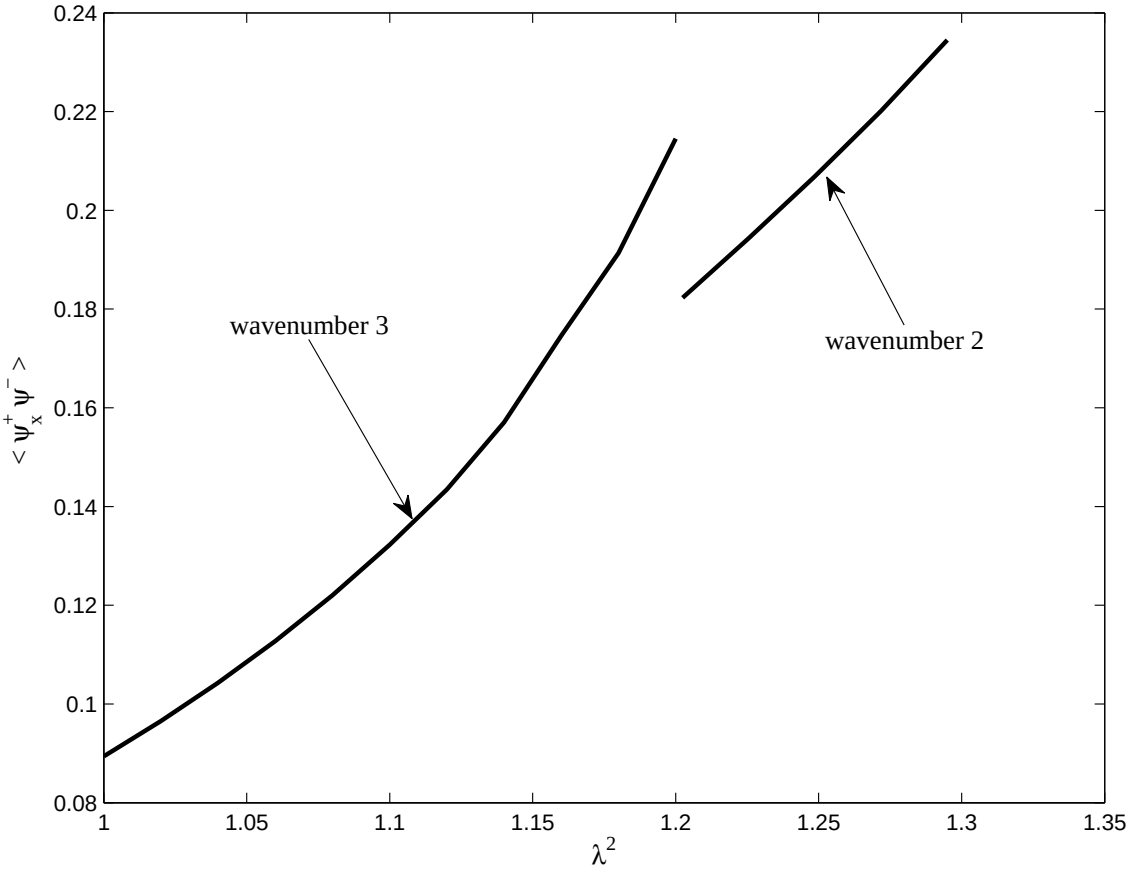

FIG. 7. For the equilibrated jets shown is the maximum heat flux $\left\langle \overline{\psi_x^+ \psi^-} \right\rangle$ as a function of Froude number, λ^2. At $\lambda^2 = 1.2$ there is an abrupt transition from a meridional wavenumber 3 jet to a meridional wavenumber 2 jet. The thermal forcing is $\Delta T = 30$ K/(10^4km) and the stochastic excitation is $f = 0.49$ mWkg^{-1} per mode. The eddy field comprises global zonal wavenumbers 1-14. The eddy damping parameters are $r_2 = 1/5$ d^{-1}, $r_R = 1/15$ d^{-1}, $r_{eff} = 1/20$ d^{-1} and the damping rate of the mean is $\overline{r}_2 = 1/5$ d^{-1} and the mean cooling is $\overline{r}_R = 1/15$ d^{-1} .

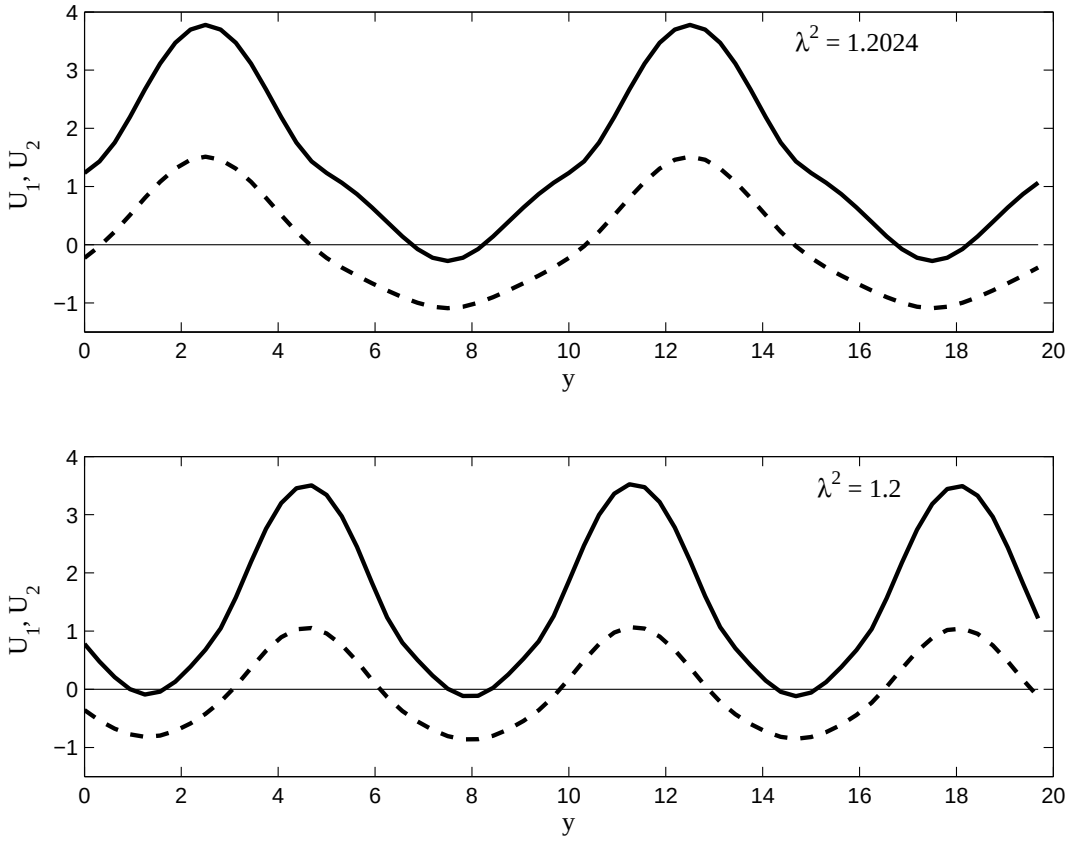

FIG. 8. Structure of the equilibrium upper layer (continuous line) and lower layer (dashed line) mean flows maintained in a channel with mean thermal forcing $\Delta T = 30$ K/(10^4 km) and stochastic excitation of $f = 0.49$ mWkg^{-1} per mode. In the upper panel is shown the meridional wavenumber 2 jet that bifurcates from the meridional wavenumber 3 jet shown in the lower panel. The parameters are the same as in Fig. 7.